Colloidal gels: equilibrium and non-equilibrium routes

2007 J. Phys.: Condens. Matter 19 323101

(http://iopscience.iop.org/0953-8984/19/32/323101)

IOP PUBLISHING JOURNAL OF PHYSICS: CONDENSED MATTER

J. Phys.: Condens. Matter **19** (2007) 323101 (50pp) doi:10.1088/0953-8984/19/32/323101

TOPICAL REVIEW

Colloidal gels: equilibrium and non-equilibrium routes

Emanuela Zaccarelli

Dipartimento di Fisica and CNR-INFM-SOFT, Università di Roma La Sapienza, Piazzale Aldo Moro 2, I-00185 Rome, Italy

E-mail: emanuela.zaccarelli@phys.uniroma1.it

Received 13 April 2007, in final form 22 May 2007
Published 17 July 2007
Online at stacks.iop.org/JPhysCM/19/323101

Abstract

We attempt a classification of different colloidal gels based on colloid–colloid interactions. We discriminate primarily between non-equilibrium and equilibrium routes to gelation, the former case being slaved to thermodynamic phase separation while the latter is individuated in the framework of competing interactions and of patchy colloids. Emphasis is put on recent numerical simulations of colloidal gelation and their connection to experiments. Finally, we underline typical signatures of different gel types, to be looked at, in more detail, in experiments.

(Some figures in this article are in colour only in the electronic version)

Contents

1. Introduction

In recent years, dynamical arrest in colloidal, and more generally in soft matter systems, has gained increasing scientific attention [1]. Colloidal suspensions have unambiguous advantages with respect to their atomic counterparts. Characteristic space and timescales are much larger, allowing for experimental studies in the light scattering regime and for a better time resolution. The large dimension of the particles allows for direct observation with confocal microscopy techniques, down to the level of single-particle resolution [2]. In addition, the 'tunability' of the system and of particle–particle interactions is almost arbitrary, as opposed to standard atomic interactions fixed by elementary chemistry. Therefore, it opens up the extraordinary possibility to 'engineer' colloidal model systems, for example by synthesizing ad hoc particles with specific properties [3] or simply changing the solution composition by appropriate additives and salt ions. This is accompanied by a great control and a fine tuning of the interparticle potential parameters [4]. The explored field of research is rapidly growing [5] to include all kinds of spherical interactions, as well as to address the role of anisotropy, either due to the shape of the particles or to the presence of different chemical subunits in the colloidal particles, the so-called 'patches', with different properties with respect to the rest of the particles.

Colloidal suspensions, despite being very complex in nature and number of components, can be well described theoretically via simple effective potentials [6]. Indeed, the solvent and additive degrees of freedom are generally much faster than those of the colloidal particles, so that they can be effectively 'integrated out'. This provides the possibility of describing the complexity of the solutions via simple effective one-component models for the colloids only, the most famous of which are the DLVO potential [7] or the Asakura–Oosawa model [8]. In this respect, from a fundamental point of view, colloidal systems and soft matter can be considered as 'ideal' model systems with 'desired interactions' to be tested with rapidly advancing experimental techniques (for a recent review of this topic, see [9]), and often closely compared with theory and simulations.

Much effort has been devoted so far to clarify the dynamical behaviour at large packing fractions, where dynamical arrest, commonly identified as a glass transition, takes place. In this respect, other reviewers have already described the state of the art [10, 11]. Here, we aim to give a perception of what happens when the system slows down and arrests at much smaller densities. An experimental review of this topic, focusing on elasticity concepts, has appeared recently [12]. Dynamic arrest at low densities, in terms of dominating mechanisms and various interplay, is still very poorly understood. A review of the low-density behaviour in attractive colloids was reported about a decade ago by Poon [13]. This work focused on the view of colloids as 'super-atoms', for which a thermodynamic description can still be applied, and mainly reported about the relation between phase separation and gelation, in particular to address the often-invoked point that a similarity, in equilibrium phase diagrams and arrest transitions, should hold between colloids and globular proteins, of deep importance because of protein crystallization issues [14, 15].

The problems in understanding deeply the low-density region of the colloids phase diagram are multiple. Experimentally, there is a zoo of results, often in contradiction with each other. Sometimes the studied systems are highly complicated to be used as prototypes of the gel transition (see for example Laponite) or to make general claims about the nature of the arrest transition and phase diagram. In other cases, the system is not well characterized enough to be sure of the responsible interactions determining some type of aggregation instead of phase separation and so on. For example, only recently the important role of residual charges on colloidal particles [16] has been elucidated in PMMA sphere gelation [17, 18]. Theoretically the situation is no better, as, in most cases, there is not yet a unifying theoretical framework

able to roughly locate and describe the colloidal gel transition, for example the Flory theory for chemical gelation [19] or the ideal mode coupling theory (MCT) [20] for colloidal glasses. MCT is applicable for low-density arrested solids only to a certain extent, for example to describe Wigner glasses [21]. Finally, the role of numerical simulations is quite important at present, since a number of models are being studied to incorporate the minimal, necessary ingredients to discriminate between gelation, phase separation, cluster or glass formation.

In our opinion, the principal question to ask is the very basic definition of what a colloidal gel is and of its, possibly existing, universal features. Moreover, it is not clear if a gel can be described in a unifying framework including glasses and non-ergodic states in general. Sometimes the terminology gel/glass is interchanged. In this review, we will try to assess under which conditions each should be used. Moreover, we will propose a classification scheme between different gelation mechanisms. In this respect, the role of interparticle potential will be important in characterizing the different gel states. We will put particular emphasis on the difference between non-equilibrium and equilibrium approaches to gelation.

In a thinking framework, the creation of an ideal model for equilibrium gels, as canonical as the hard sphere model for glasses, would be important for future studies. Very recently, some efforts towards the individuation of the basic ingredients that are necessary to design such a model have been carried out. Strong evidence, from experiments [22] and simulations [23, 24], has proven that for hard-core plus spherically symmetric pairwise attractive potentials, arrest at low density occurs only through an interrupted phase separation. In the limit of very large attraction strength and very small density, this scenario crosses continuously to diffusion-limited cluster aggregation (DLCA) [25]. Modification of simple attraction is invoked to produce gelation in equilibrium. This turns out to be the case when long-range repulsion, induced by excessive surface charges in solution, complements the short-range depletion attraction [26], as well in the new family of patchy [27] or limited-valency potentials [28]. The present review will try to describe some of the models and their predictions for gelation, focusing mainly on recent advances in modelling and simulations. Finally we will try to characterize, within the limits of the present knowledge, the basic features of the different encountered gels in connection to experiments. Our aim is to provide a reference framework for future understanding of this complicated state of matter, that is ubiquitous in applications, and frequent in everyday life from the kitchen table to our own body.

2. Definitions and scope

To present a coherent picture of the state of the art in the field of colloidal gelation, we introduce and classify in this section different phenomena that have similarities, interplay, or are at the essence of colloidal gelation. In particular, we start by discussing chemical gelation and percolation theory. Then we describe physical gels and we illustrate the gel-formation process with respect to percolation and phase separation. We also briefly mention DLCA gels. We will emphasize the role of the 'bond lifetime' as key concept to identify a gelation mechanism. We illustrate equilibrium and non-equilibrium routes to physical gelation, introducing the concept of 'ideal gels' and drawing typical phase diagrams as a reference for the different types of systems. Two brief paragraphs will conclude this section, with the specific goals to (i) clarify the role of percolation towards gelation and other types of arrested low-density solids and (ii) highlight the repulsive and attractive glass transition at high densities. Both these topics are very relevant to the following discussion, especially to understand their relation, in properties and location, with respect to the phase diagram and (eventually) gel formation.

In section 3, we focus on the role of the bond lifetime as the parameter connecting chemical to physical gelation, reporting results from numerical models which have focused on this

aspect. In section 4, we will discuss three different routes to gelation: (i) non-equilibrium gelation as arrested phase separation; (ii) equilibrium gelation resulting from a competition between short-range attraction and long-range repulsion; (iii) equilibrium (and ideal) gels made of particles with patchy (or directional) interactions. In section 5 we try to individuate common and different signatures of the three types of gels in connection to experimental observations (past or future). Finally, we draw our conclusions and perspectives of future studies.

2.1. Basic definition of a gel

Let us start with the basic definition of a gel from the Encyclopædia Britannica: *coherent mass consisting of a liquid in which particles are either dispersed or arranged in a fine network throughout the mass. A gel may be notably elastic and jellylike (as gelatin or fruit jelly), or quite solid and rigid (as silica gel)* [29]. From this general definition it follows that a low-density disordered arrested state which does not flow but possess solid-like properties such as a yield stress is commonly named a gel. Similarly to glasses, the gel structure does not show any significant order and, in this respect, it is similar to that of a liquid. However, for dilute systems, a gel often displays a large length scale signal associated with the fractal properties of its structure. The terminology of sol–gel transition refers to a liquid mixture where solute (sol) particles (ranging from monomers to biological macromolecules) are suspended in a solvent. Initially the sol particles are separated, but, under appropriate conditions, they aggregate until a percolating network is formed. In the following the conditions under which such percolating network can be defined as a gel will be discussed. Colloidal gels are often formed by particles dispersed in a liquid solvent. However, in polymers and silica gels the solvent is not a liquid or it is missing.

2.2. Chemical gelation and percolation

Chemical gelation studies were initiated in the framework of cross-linking polymers, whose gelation transition was associated with the formation of an infinite network with finite shear modulus and infinite zero-shear viscosity. At the gelation point, the system stops flowing. One possible example of polymer gel-forming systems is provided by epoxy resins [19]. In these systems, polymer chains grow step-wise by reactions mediated by end-groups or cross-linkers (step polymerization). As the reaction takes place, chemical (hence irreversible) bonds between different chains are formed. If the (average) functionality of the monomers is greater than two, to allow the establishment of a branched structure with junction points, a fully connected network, spanning the whole space, is built [30] and a gel is obtained. Another example is rubber, whose gelation process is usually called vulcanization, where entangled polymers are not bonded at first, and, with time of reaction, covalent bonds are chemically induced.

The irreversible (chemical) gelation process is well described in terms of percolation theory, since—due the infinite lifetime of the bonds—the gel point coincides strictly with the appearance of an infinite spanning network. The mean-field theory of percolation was developed by Flory [31] and Stockmayer [32, 33], under the following two assumptions: independent bonds and absence of bonding loops. Each possible bond is formed with a probability p and the percolation threshold is identified in terms of a critical bond probability p_c, analytically calculated on the Bethe lattice [31, 34]. Close to p_c, the cluster size distribution $n(s)$ is found to scale as a power law of the cluster size s: $n(s) \sim s^{-\tau} f[s^{\sigma}(p - p_c)]$, while the mean cluster size $S \equiv \sum s^2 n(s)/[\sum s n(s)]$ is found to diverge at percolation as $S \sim (p - p_c)^{-\gamma}$. The probability of belonging to the spanning cluster P_∞ is found to grow from the transition as $P_\infty \sim (p - p_c)^{\beta}$. Finally, the cluster radius of gyration R_g is found to

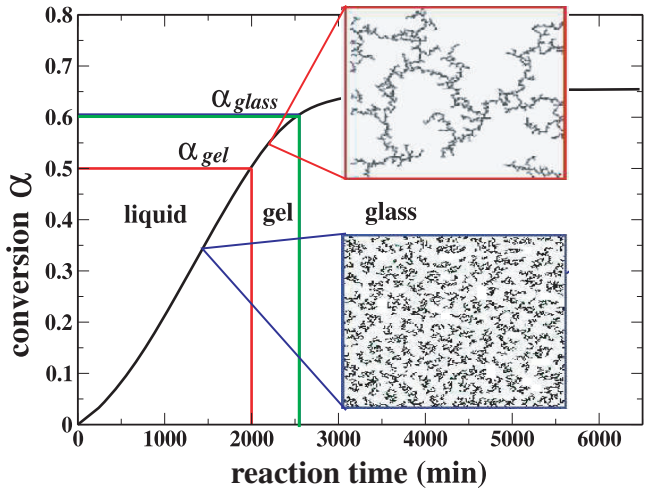

Figure 1. Chemical conversion α, indicating the fraction of formed bonds during a chemical reaction, versus reaction time. It commonly saturates at a finite value well below unity. Before reaching a plateau value, the system encounters the gel transition at $\alpha_{\rm gel}$ and the glass one at $\alpha_{\rm glass}$. The curve refers to a mixture of epoxy resins with different functionalities. The images show a representation of the liquid phase and of the gel network. Note that different scales are used for resolution of the two images: the particle volume fraction does not change along the reaction. Courtesy of S Corezzi.

scale with the cluster size as $R_{\rm g} \sim s^{1/d_{\rm f}}$, where $d_{\rm f}$ is the cluster fractal dimension. Here, τ, γ, β and σ are universal exponents satisfying appropriate scaling relations, as $\gamma = (3-\tau)/\sigma$ and $\beta = (\tau-2)/\sigma$, while $f(z)$ is a system-dependent scaling function [34]. In 3D, the exponents have been calculated numerically for many systems, resulting in $\tau = 2.18, \sigma = 0.45$ and $d_{\rm f} = 2.53$, which are the exponents of the random percolation universality class.

Percolation is defined in term of bonds, i.e. it is based on the connective properties of the system. It does not require information on the physical properties of the bond, on the temperature dependence of the bond probability or, even more importantly, on the lifetime of the bonds as well as of the spanning cluster. In this respect, its extension to non-covalent (non-permanent) bonds requires caution.

In the case of chemical bonds, a clear distinction can be formulated between chemical gelation and chemical vitrification. As shown in figure 1, with the proceeding of a polymerization process, an increasing fraction of bonds α, commonly named chemical conversion, is formed. Gelation is found at the time of reaction where the systems stop flowing. At this point the system percolates and only the fraction $\alpha_{\rm gel}$ of possible bonds is formed, which can be well predicted by Flory theory [19]. With further proceeding of the reaction, other bonds are formed until a point where α saturates to a plateau value, well below the fully connected state ($\alpha = 1$). This indicates that the system becomes trapped into a metastable minimum of the free energy and undergoes a glass transition at the typical conversion $\alpha_{\rm glass}$. In this case, the system becomes non-ergodic, the density auto-correlation function displays a plateau in time and the structural relaxation time becomes larger than the experimental time window [35, 36], as found in standard glasses. A length-scale dependent analysis of the chemical gel and glassy states should be able to discriminate between the two cases. Indeed, while the glass is non-ergodic at all relevant length-scales, the gel only has a correlation, dictated by the infinite network, strictly at $q \to 0$, while all other length-scales retain a quasi-ergodicity.

Experimental and simulation works on chemical gelation have reported [37–41] (i) a slow relaxation approaching the gel transition, that can be well fitted by a stretched exponential decay, and (ii) a power-law decay of the density and stress auto-correlation functions close to percolation. An experimental study of the dynamical behaviour well within the gel region is also performed in [39], where the power-law decay is also found in the gel phase for q-values well in the diffusive regime. Given the limited investigated range in q and in gel states, no extensive characterization of the wavevector dependence of the gel and percolation transition was performed, also in relation to the evolution of the non-ergodic properties approaching the glass transition.

2.3. Physical gelation

Physical gels are gels in which bonds originate from physical interactions of the order of $k_B T$, so that bonds can reversibly break and form many times during the course of an experiment. This provides a fundamental difference in the nature of chemical with respect to physical gels. The latter are usually formed by colloidal and soft particles as well as associative polymers, and bonds are induced via depletion interactions, hydrogen bonds and hydrophobic effects to name a few. This difference allows us to classify generally as chemical gels those characterized by irreversible bond formation, and as physical gels those in which the bonds are transient, i.e. are characterized by a finite (although large) lifetime.

Non-exhaustive examples of transient gel-forming systems are the following: colloid–polymer mixtures [42–45], in which polymers act as depletants, and hence polymer concentration c_p controls the attraction strength; colloidal silica spheres that are sterically stabilized by grafting polymer chains onto their surface [46–50], where temperature, changing the solvent quality of the polymer chains, acts as the control parameter for effective adhesive attractions between the colloidal spheres; telechelic micelles with functionalized end-groups [51–53] or a ternary mixture of oil-in-water microemulsion in suspension with telechelic polymers [54], where bridging of micelles is provided by hydrophobic end-caps; among gel-forming protein systems, the case of sickle cell haemoglobin [55, 56], where attraction should be as in typical globular proteins short range, probably patchy, and arising from a combination of hydrophobic effects and van der Waals attraction.

In the framework of thermoreversible gelation for associative polymers, a long-standing debate involves the association of the percolative (network-forming) transition to a thermodynamic transition. This question arises naturally from the different assumptions implied respectively in the Flory and in the Stockmayer approach in the post-gel regime. A recent review focused on this question [57] and suggested, based on several studies of different associating systems, that the gel transition is not thermodynamic, but rather *connective* in nature. In this review, we provide evidence that no signature of a thermodynamic transition is found in colloidal gelation, a result consistent with the finite lifetime of the bonds. Moreover, we point out that, in general, when the bond lifetime is much shorter than the experimental timescale, the establishment of a network, i.e. percolation, is not even associated with a dynamic transition.

In standard percolation studies, the bond lifetime, and hence the lifetime of the spanning cluster, is not taken into account. For chemical gels, the bond lifetime is infinite and thus percolation theory has been the theoretical framework for describing the gel transition. In the case of chemical bonds, where bond formation and bond duration are coupled, the percolation concept is connected to the dynamics and thus it can describe the chemical gelation transition. For colloidal gels, bonds are transient. Clusters break and reform continuously. Percolation theory can thus be applied only to describe static connectivity properties. Neglecting dynamic

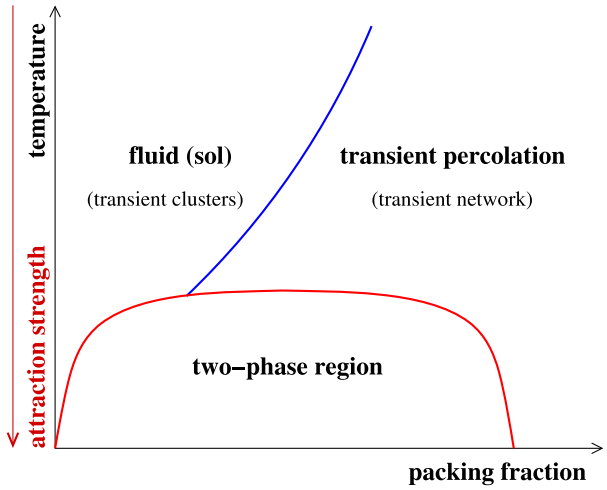

Figure 2. Schematic picture of the percolation transition in physical gels, where the formation of a transient network does not have any implication for gelation.

information, it is still possible to locate the line in the phase diagram where a spanning transient cluster first appears, which plays the role of percolation transition locus. Analysis of the cluster size distribution and of all other percolation observables (S, P_∞, R_g) close to such a line are consistent with the universality class of random percolation [34, 58].

A schematic plot of the phase diagram for a simple attractive potential, including beside the phase separation locus also the percolation line, is shown in figure 2. No dynamical ingredients are taken into account within this picture, and hence no information on the location of the arrested states is provided. Only if the lifetime of the bonds close to the percolation locus is longer than the experimental observation time would it be possible to conclude that the system becomes non-ergodic at the percolation line. Among the studies pointing out the irrelevance of the percolation transition for reversible gelation was a theoretical description of thermoreversible gelation for associating polymers by Rubinstein and Semenov [59], soon followed by a lattice model simulation by Kumar and Douglas [60].

The colloidal gel-forming systems are often based on spherically symmetric attractive potentials. One famous example is the Asakura–Oosawa (AO) [8] effective potential for colloid–colloid attraction entropically induced by the polymers. Bonds can here be defined between any pair of particles with a relative distance smaller than the attraction range. When attraction strength is increased, the system prefers to adapt locally dense configurations, so that energy can be properly minimized. Under these conditions, a liquid condensation (a colloidal liquid) is favoured, as discussed in more detail below. The presence of a phase-separation region in the phase diagram is thus often intimately connected to the presence of a percolation locus [61, 62].

2.4. Interplay between phase separation and physical gelation

Percolation in physical gel-forming systems does not correspond to gelation due to finite bond lifetime. Long-living bonds necessarily require large attraction strength. In systems in which the hard-core interaction is complemented by spherically symmetric attraction, very large attraction strengths not only increase the bond lifetime but also inevitably lead to the onset of liquid–gas (colloid rich–colloid poor) phase separation. We can rationalize the tendency to

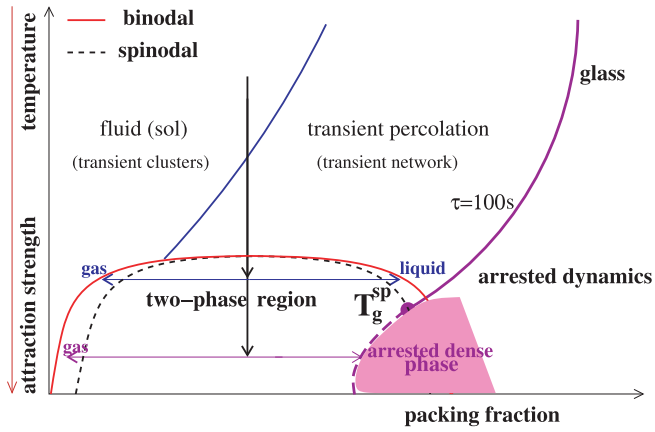

Figure 3. Schematic picture of the interrupted phase separation or arrested spinodal scenario. A quench into the two-phase region may lead to an arrest of the denser phase. It is not yet clear how the glass line continues within the spinodal region. The figure shows the case where the density fluctuations freeze before they reach the final spinodal value, a scenario that is supported by a study on lysozyme [67]. Alternatively, the glass line might merge with the spinodal on the high density branch.

phase separate through Hill's work on liquid condensation in term of physical clusters [63]. Indeed, the free energy F_N of a cluster of N particles can be written as a contribution of a bulk and a surface term, respectively proportional to N and to $N^{2/3}$. Thus $F_N/N = f_{\rm bulk} + \gamma N^{-1/3}$, where γ is proportional to the surface tension and $f_{\rm bulk}$ is the free energy per particle in bulk conditions. If $\gamma > 0$, then F_N/N is minimized for $N \to \infty$ and hence a condensed liquid phase is expected. At sufficiently low T, where entropic terms can be neglected, $\gamma \propto (e_{\rm surface} - e_{\rm bulk})$, where $e_{\rm surface}$ and $e_{\rm bulk}$ are the energy of a particle on the surface and in the interior of a cluster respectively. For spherically symmetric attractive potentials $e_{\rm bulk} < e_{\rm surface}$ and hence $\gamma > 0$ (see for example the calculation for cluster ground state energy for various widths of attraction from Lennard-Jones to narrow wells [64, 65]), so that lowering the temperature will always induce phase separation. If $\gamma \leqslant 0$ [66] a bulk liquid–gas separation will be disfavoured. We will analyse the separate cases $\gamma < 0$ and $\gamma \simeq 0$ later on.

On the basis of these considerations we can suggest a first crucial distinction between different types of arrest at low density by discriminating whether the system undergoes gelation with or without the intervening of phase separation.

If the phase separation boundary is crossed before dynamical arrest takes place (for example through a quench inside the spinodal decomposition region) the system will experience liquid condensation. The coarsening process will induce the formation of dense regions, which might arrest due to the crossing of a glass transition boundary. In this case we talk of 'arrested (or interrupted) phase separation' or 'arrested spinodal decomposition' [23, 68]. This route to gelation is a non-equilibrium route, as it is made possible through an irreversible process, i.e. spinodal decomposition, and it is pictorially represented in figure 3, and discussed in detail for short-ranged attractive colloids, in particular colloid–polymer mixtures, in section 4.1.

2.5. DLCA gels

A remarkable case of arrested spinodal mechanism is that of DLCA [25], that is realized when a very low-density colloidal system is quenched to a state point with large attraction

strength, combining in this limit aspects of chemical and physical gelation. Indeed, in this limit, attraction is so large that bonds are effectively irreversible. The aggregation process is mediated by diffusion of the growing clusters, which irreversibly stick when touching, forming a well characterized fractal structure (with $d_f \simeq 1.75$). Arrest is achieved by inhomogeneous filling of all available space with clusters of progressively smaller density. The percolation transition is here mediated by clusters, rather than particles as in chemical gelation.

Several experimental studies have focused on gelation in the DLCA limit [69–71]. In these strongly aggregating colloids, the bond energy is much larger than $k_B T$. These types of gels are found to exhibit fractal properties and aging dynamics [72, 73]. Interestingly, several types of fundamental questions on the internal dynamics, restructuring and limits of stability of such low-density gels can be tackled by these kinds of studies [74–77]. In these types of gels, phase separation is kinetically interrupted by the freezing of the bonds, hence we can also consider these gels to belong to the category of 'out-of-equilibrium' gels.

Also, many numerical studies have addressed DLCA, at first onto a lattice with particular interest in understanding the cluster properties and the fractal dimension [78–80, 25, 81]. Later on, studies have addressed the full gelation process, to also examine the fractal properties and structure of the gel [82, 81]. To do so, off-lattice realizations of DLCA were employed [83–85], to allow for a more realistic characterization of the structure of the clusters as well as of the percolating network.

2.6. Equilibrium approaches to gelation

If phase separation is not intervening (for example via the realization of the condition $\gamma \leqslant 0$ in Hill's formalism) the system is able to form a stable particle network, through a series of equilibrium states. We call this scenario 'equilibrium gelation', since the gel state is reached continuously from an ergodic phase, always allowing an equilibration time, much longer than the bond lifetime, for the system to rearrange itself. It is important to point out that the experimental determination of a gel transition requires an arbitrary definition of timescale, in analogy with the glass case. The glass transition is commonly signalled with the point where the viscosity of a glass-forming system becomes larger than typically 10^{13} poise, or equivalently, when the non-ergodic behaviour persists for an observation timescale of 10^2 s.

Also in the case of gels, the dynamical arrest process will be strictly connected to the observation time window. Indeed, the bond-lifetime being finite, there always exists a longer timescale over which the system will eventually relax. Therefore, it is useful to adopt an 'operative' definition of gelation transition. We could define, similarly to glasses, an equilibrium gel as a low-density state when the percolating network lifetime is larger than 10^2 s. Of course, if one waits a long enough time, i.e. more than this established minimal lifetime of a percolating network, the system will possibly still restructure itself, due to bond rearrangements. Hence, strictly speaking, a true ideal gel transition should only take place at infinite network lifetime. When the bond lifetime is governed by an Arrhenius dependence on the attraction strength, the ideal gel state would arise at infinite attraction strength (vanishing T for temperature-activated bonds). In the following we will refer to equilibrium 'gel' states as those approached continuously from the fluid phase and exhibiting a long (even if not infinite) lifetime, retaining the 'ideal gel' concept only to those extrapolated states where lifetime becomes infinite. In these respects, percolation is a necessary pre-requisite (since the infinite spanning network is present only after percolation is reached) but it is not sufficient for defining a gel state.

We can distinguish again two different topological phase diagrams for equilibrium gelation. Firstly, in one case the phase separation is pushed towards higher attraction strength

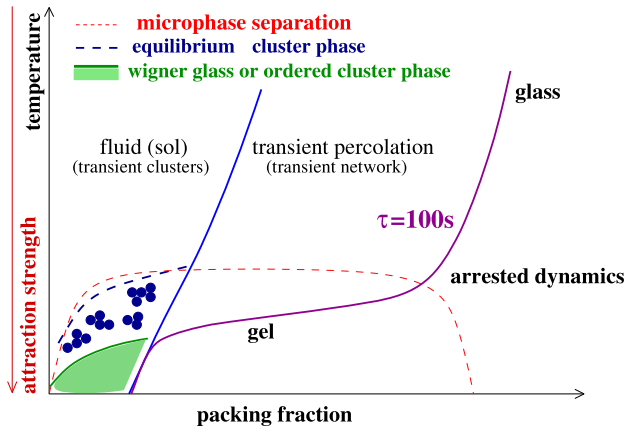

Figure 4. Schematic picture of the stabilization of an equilibrium cluster phase and gel, through the inhibition of the phase separation region by an enhanced bond lifetime, when additional long-range repulsion are taken into account. Equilibrium clusters are formed due to the microphase separation. At low T and low ϕ (filled area), such clusters form either a disordered (Wigner glass) or an increasingly ordered phase (cluster crystal, columnar phase) depending on residual cluster–cluster interactions. At low T and larger ϕ, gelation results as percolation of the long-lived clusters.

[86] and can be replaced by microphase separation. This can be achieved through an enhancement of the bond lifetime, for example by considering various sorts of stabilizing barrier in the potential with [87] or without [88–92] a clear microscopic interpretation. A similar effect can be obtained when considering the effects of residual charges onto colloidal particles (or proteins) in suspension, which give rise to an additional long-range repulsion in the effective interaction potential. In this case, the condition $\gamma < 0$ in Hill's terms [63] can be realized through the addition of a sufficiently long-ranged repulsion, whose range is controlled by the Debye screening length ξ. Hence, a finite optimal size of clusters N^* exists which minimizes the free energy (microphase separation), generating a so-called equilibrium cluster phase [16, 21, 93]. This behaviour will be discussed in detail in section 4.2. For the present description, such a modification of the potential opens up a window of stability for the equilibrium gel by pushing the phase separation at larger attraction strengths. In the microphase separating region, at low density, equilibrium clusters are found, merging somehow into a percolating network at larger densities. A qualitative picture is proposed in figure 4, where the $\tau = 100$ s line signals the slow dynamics, connecting the gel and the (attractive) glass line at higher densities. The only case where a similar phase diagram has been discussed for a wide range of densities, encompassing both gel and glass states, is found in the works of Puertas *et al* [89, 94]. Although the authors play down the role of the repulsive barrier, which is just employed ad hoc to prevent phase separation, they find evidence of a gel phase at an intermediate packing fraction $\approx$0.40, which, by MCT analysis, is compatible with attractive glass features [95, 96]. Finally, we note that, if ξ is sufficiently long, the phase separation can be completely absent (as in the limit of unscreened Coulomb repulsion), so that at very low ϕ, below the percolation threshold, and very low T, a Wigner glass of clusters is expected [21].

The other case that can lead to equilibrium gelation is realized when a mechanism for inhibition of phase separation not only to lower temperatures, but most importantly to lower packing fractions, is at hand. This is achieved by inducing directional interactions between colloidal particles, preferably of low coordination. We will see that lowering the (average) coordination number is the essential condition to push the critical point to lower and lower packing fraction. In this case, we can consider that $\gamma \to 0$ in Hill's formalism, as at low T

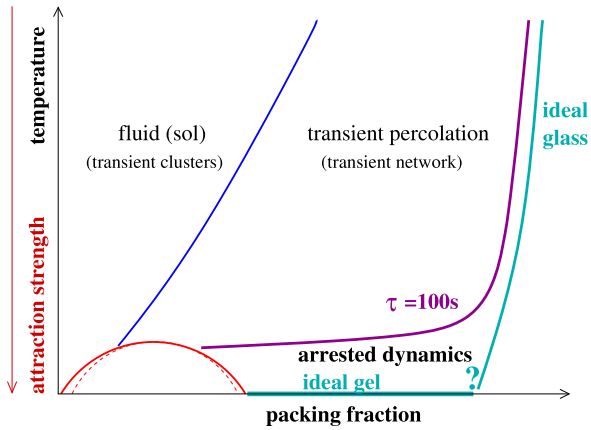

Figure 5. Schematic picture of the shift to lower packing fractions of the phase separation region and emergence of an equilibrium gel phase, as well as of the ideal gel phase at $T = 0$. The question mark refers to the unknown details of the crossover from gel-to-glass dynamics.

the driving force for compact aggregation becomes very small, since the energy is the same in the interior and on the surface of a cluster, thus enhancing saturated network structures. In this case, a completely new topology of the phase diagram is found. A wide region of stability of an equilibrium network, to become a gel at lower and lower T, opens up at low/intermediate densities. Through a careful equilibration procedure down to very low T, almost-ideal gel states may become accessible. This new topology of the phase diagram and arrest transitions is sketched in figure 5, where the line of arrest, again drawn as a $\tau = 100$ s line, joins the slow gel states with the glassy states at large ϕ, but in truth these two lines are distinct and the ideal gel and glass lines are reported, with a question mark about the nature of the crossover/meeting between the two lines. We will elucidate this scenario in the framework of patchy models in section 4.3.

2.7. Question: is percolation strictly necessary to form a gel?

We have seen so far that percolation is not a sufficient condition for physical gelation. However, it should be at least a necessary condition, if one follows the idea that a gel arises from a stable percolating network. Within this picture, attraction should be a necessary ingredient for gel formation. However, some systems may form arrested states at extremely low densities, and their properties be not at all related to percolation. This happens primarily in systems with sufficiently long-range repulsion, that in the end acts as the stabilizing mechanism for arrest. Essentially two classes of systems that we are aware of are found to belong to this category. Firstly, soft or ultrasoft systems, like star polymers, micelles and other aggregates where effective interactions between different objects can be slightly repulsive close to contact, essentially for entropic reasons. When two of these objects become close enough that the end-monomers feel the effects of self-avoidance, these systems become solid. Secondly, highly charged systems at low screening conditions that, independently from the presence of a short-range attraction, feel at longer distances (comparable to the average distance dictated by number density) a strong repulsion. Both these classes of systems can form a low-density non-ergodic disordered solid, that is governed by repulsive interactions. The prototype model for such a low-density arrest transition is the Yukawa potential, which describes both star-polymer-like systems and charged colloids in suspensions. For charged systems, the arrested state is usually

called a Wigner glass and can be formed by particles (in purely Yukawa systems) [97, 98] or by clusters (in the presence of an additional short-ranged attraction) [21], or perhaps by both in different regions of the phase diagram as recently speculated in Laponite suspensions at low ionic strength [99, 100]. In star-polymer and soft micellar systems, the arrest transition is described in the literature as a gel or jamming or glass transition [101–105] and it can be theoretically interpreted both in an effective hard-sphere picture [106] and in a purely Yukawa treatment [107]. The question that naturally arises is whether these states should be considered gels or glasses in general terms. It is certainly, once again, a matter of definition how to interpret the arrest, so that the resulting arrested state is often named a gel without discrimination of whether its origin is purely network formation or not. This happens primarily because it is sometimes hard to call glass a solid observed at, for example, a packing fraction of few per cent, where particles are very far from each other. We may propose that a gel should necessarily have attraction as the leading mechanism for gelation, while a glass can be driven either by repulsion (hard-sphere or Wigner glass), or by attraction just in the high-density region (attractive glass).

Hence, while in theory and simulations, the knowledge of the governing interactions would render it easy to discriminate a gel from a glass at low density, in experiments, if the interactions at hand are not clear for example in the case of Laponite, this can be a hard task. An interesting test that could be performed experimentally to provide an answer to this question could be a sort of 'dilution test'. The low-density solid could be smoothly diluted (without being altered in nature) and if persisting, at least for some dilution range, attraction should be identified as a relevant mechanism, thus invoking a gel state, while if breaking apart repulsion could be the responsible mechanism for a Wigner glass state. Of course, care should be taken that, for example in charged systems, the counter-ion concentration is not dramatically affected by dilution in order to avoid a drastic change in the Debye screening length ξ, which governs the repulsive glass state.

2.8. Attractive and repulsive glass transition and mode coupling theory

To correctly locate and interpret the different gel lines, we need to clarify the high-density behaviour for short-ranged attractive colloids and in particular to address the two glass transitions arising in these systems: repulsive and attractive glasses. This issue has been recently reviewed by other authors [10, 11, 9] and, to avoid redundancy, we report here only a brief summary of the main findings.

The canonical model for glass transition in colloids is the hard-sphere (HS) model, realized experimentally with PMMA particles in an appropriately index-matched organic solvent (toluene +*cis*-decaline) [108–110]. Its study allowed the first direct comparison between MCT [20] of the ideal glass transition and experiments. MCT provides equations of motion for the dynamical evolution of the (normalized) density autocorrelation functions,

$$F_q(t) = \frac{\langle \rho_q^*(0)\rho_q(t)\rangle}{NS(q)} \tag{1}$$

where N is the number of particles, $\rho_q(t) = \sum_{j=1}^{N} \exp(\mathrm{i}\mathbf{q}\cdot\mathbf{r}_j(t))$ is the Fourier transform of the local density variable and $S(q) = \langle|\rho_q|^2\rangle/N$ is the static structure factor. Despite uncontrolled approximations in its derivation [20, 111], the theory is able to predict the full dynamical behaviour of the system, starting only from the knowledge of equilibrium properties, such as $S(q)$ and the number density $\rho = N/V$. For simple pair interaction potentials, the use of integral equation closures can be used to obtain a good estimate of $S(q)$. Alternatively, the 'exact' $S(q)$ can directly be evaluated from numerical simulations. We remind the reader of previous reviews [20, 11] for details of the equations and predictions of the theory.

Light scattering measurements at different angles directly provide the same observable $F_q(t)$ to be compared with MCT. For HS, a quantitative comparison was carried out by van Megen *et al* [109] for different values of the packing fraction $\phi = \pi\rho\sigma^3/6$, with σ being the diameter of the particles, and of the scattering vector q. Taking into account a shift of the glass transition point—roughly $\approx$0.58 in the experiments, while it is underestimated by 10% within MCT—they found a strikingly similar behaviour between theory and experiments and were able to verify the main predictions of MCT. Avoiding crystallization thanks to the intrinsic polydispersity of colloidal particles, the HS glass transition is approached upon super-compressing the system, the packing fraction ϕ being the only control parameter. Hence, a typical two-step relaxation in $F_q(t)$ develops with increasing ϕ. An initial microscopic relaxation, corresponding to the vibrations of particles around its initial configuration, is followed by a plateau which becomes longer and longer upon increasing ϕ. The presence of a plateau indicates that particles are trapped in cages formed by their nearest neighbours. The height of the plateau, coinciding with the long-time limit of $F_q(t)$, is defined as the non-ergodicity parameter f_q. When the particle is capable of breaking such a cage and escaping from its initial configuration, ergodicity is restored and a final relaxation is observed, named α-relaxation. Otherwise, the system remains trapped in a non-ergodic state, i.e. a glass (at least on the timescale of experiments, as said above typically of 10^2 s). A similar picture emerges from examining the mean squared displacement (MSD) $\langle r^2(t)\rangle$, which also displays an intermediate plateau between short-time Brownian diffusion (or ballistic motion for Newtonian dynamics) and long-time diffusion. The plateau in the MSD allows us to obtain a direct measurement of the cage in which particles are confined, and for HS glass it is of the order of 10–15% of the particle diameter.

These experiments opened up the way for a systematic application of MCT in colloidal systems. The next step was to consider the effect of a short-range attraction complementing the hard-core repulsion. This type of modification of the interactions can be easily produced in hard-sphere colloidal suspensions simply by adding non-adsorbing polymers, thereby inducing an effective attractive force between the colloids via depletion interactions. This has been known since the pioneering works of Asakura and Oosawa [8] and Vrij [112]. It turns out that the width of the attraction Δ can be simply controlled by changing the size of the polymers and its magnitude simply by changing the polymer concentration. New unexpected features emerged from the study of short-ranged attractive colloids within MCT [113–115]. These results were found to be independent of the detailed shape of the short-range attractive potential (SW, hard-core attractive Yukawa, AO etc), as well as of the approximation used to calculate $S(q)$. They can be summarized as follows and pictorially represented in figure 6, redrawn from [116].

At high densities, two distinct glassy phases are identified. Along a fixed isochore with $\phi > \phi_g^{HS}$, where ϕ_g^{HS} is the HS glass transition threshold, the HS glass is found at high temperatures, also named repulsive glass. At low temperatures, a new glass, named attractive glass, appears. This is induced by the attractive bonds between the particles. In between these two glasses, at intermediate temperatures, there is a re-entrant pocket of liquid states, which exists at higher ϕ with respect to the HS glass. The phenomenon at hand is achieved when the range of attraction is sufficiently smaller than the typical localization length of an HS glass. In this situation, decreasing the temperature, some particles will tend to get closer within the attractive range, thus opening up free volume in the system. In this way, dynamics is speeded up by an increase of attraction strength. A further decrease of temperature localizes most particles within the bonds, until they are trapped within the bond distance. Here, a second glassification process arises driven by energy, as opposed to the repulsive glass, which is driven by entropy. It is therefore the competition between these two glasses that determines the

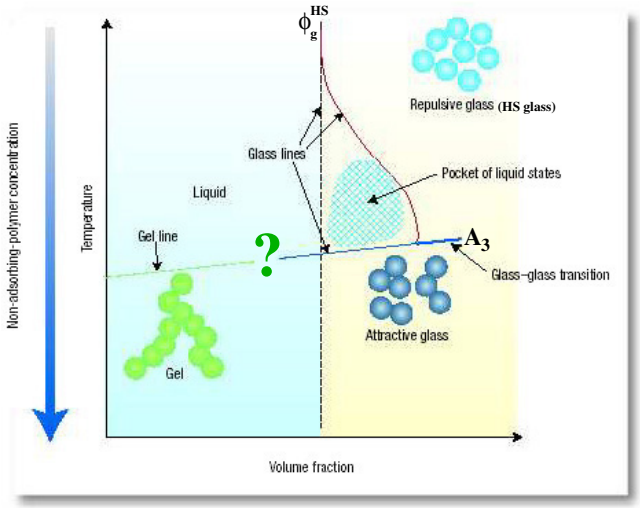

Figure 6. Cartoon of the re-entrant repulsive and attractive glass transitions at high density for short-ranged attractive colloids. Adapted with permission from Macmillan Publishers Ltd: [116], copyright 2002.

re-entrance in the glassy phase diagram as well as an anomalous dynamical behaviour for these systems [116, 117].

Confirmation of the re-entrant liquid regime was provided by several experiments on different systems [118–125] and by numerical simulations [88, 126, 127, 89], thereby making very robust the MCT predictions for this class of potentials. The two glasses can be differentiated by their respective non-ergodicity factors and localization lengths [118, 127]. The attractive glass is confined by the short-ranged attractive bonds, implying that f_q is consistently higher than the HS one at all wavevectors, and that the MSD plateau is of order $\Delta^2 \ll (0.1\sigma)^2$. Moreover, the two glasses are characterized by utterly different rheological properties [128–130, 50]. In figure 6, the attractive glass line is virtually extended to low densities to indicate a possible merging to the gel line. We will address this point in the routes to gelation section.

When the two glass lines meet, a discontinuous glass–glass transition is predicted. It is to be noticed that this is a purely kinetic transition, given the fact that $S(q)$ are virtually identical at the transition [92, 130]. The glass–glass transition line terminates into a higher order singularity point [20] (A_3), beyond which the two glasses become indistinguishable and the transition is continuous. There exists a particular state point (ϕ^*, T^*, Δ^*) for which the higher-order singularity point coincides with the crossing point of the two glass lines. In this case, the glass–glass line becomes just a single point, and the higher-order singularity is approached from the liquid side, and not buried within the glassy regime. Associated with such higher-order singularity, MCT predicts a new type of dynamics for the intermediate scattering function and the MSD [131, 132] that was confirmed in numerical simulations [133]. Instead of observing a two-step relaxation with an intermediate plateau, the relaxation is governed by a logarithmic behaviour, arising from the competition of the two glassy states. Thus, the MSD displays a subdiffusive regime $\propto t^\alpha$, with $\alpha < 1$ being state-point dependent, and $F_q(t)$ can be fitted in terms of a polynomial in $\log(t)$. The influence of the A_3 higher order singularity on the dynamics is also found in the re-entrant liquid region; thereby, numerous confirmations of logarithmic behaviours have been provided in experiments and simulations [120, 134, 88].

Finally, when the range of attraction increases, the two glasses tend to become identical [115] as there is no distinction between the bond (energetic) cage and the geometrical (free-volume) cage. For very large Δ, attraction tends to stabilize the glass to lower densities and the slope of the glass line in the (ϕ, T) plane for large T is opposite to that reported in figure 6. A detailed review of the glassy phase diagram and associated dynamics has already been reported in [9, 11].

3. Connecting chemical to physical gelation: the bond lifetime as a tunable parameter

To describe physical gelation, models were developed at first by building on existing knowledge about DLCA and chemical gelation. The reversibility concept was initially introduced to study thermoreversible polymer gels [135] or to address the properties of a reversible DLCA-like process in 2D [136], where a different structure of the clusters, e.g. a different fractal dimension with respect to irreversible formation, was found.

To our knowledge, the first study where the concept of a finite bond lifetime was introduced, to mimic colloidal gel formation, is due to Liu and Pandey [137]. On a simple cubic lattice, the dynamics of aggregation of functionalized sites was followed under two different conditions: irreversible aggregation, and reversible aggregation, where reversibility was modulated by a finite bond breaking probability p_b. The results of such study were limited to a shift of the gel transition with varying p_b, associated with different scaling properties and exponents. Building on DLCA-like models, Gimel *et al* [138, 139] studied the interplay between gel formation and phase separation for a 3D lattice model with Monte Carlo dynamics, where a bond probability p_b is assigned to neighbouring sites.

More recently, a lattice model was extensively studied by Del Gado and coworkers [41, 140] to connect chemical and colloidal gels by means of a tunable bond lifetime parameter. They studied tetrafunctional monomers with a fraction of randomly quenched bonds, mimicking the irradiation process of a polymer solution that induces chemical bonds. The bonds are formed with probability p_b and are permanent in the case of chemical gelation, while they can be broken with a finite probability in the case of colloidal gelation. Fixing the bond lifetime to τ_B, bonds are broken with a frequency $1/\tau_B$ so that a constant number of bonds is always present, in order to compare dynamics for permanent and transient bonds. In the analysis of the decay of the density correlation functions, the authors observe a power-law decay close to percolation for irreversible bonds, as found in experiments for chemical gels. However, when τ_B is finite, a crossover to a standard glassy dynamics is found, with a typical two-step decay well described by the MCT Von Schweidler law [20]. A plot of the α-relaxation time for different values of bond lifetimes at various ϕ (see figure 2 in [41]) reveals quite strikingly this crossover, which takes place at larger ϕ with increasing τ_B. Very recently, the same authors also proposed to use this framework to explain the viscosity behaviour with density of rheological measurements for L64 block copolymer micelles [141].

A revisiting of the model by Del Gado *et al* in terms of a simple off-lattice model was proposed by Saika-Voivod *et al* [91]. This model consists of a modification of a simple SW model, adapted to a binary mixture to suppress crystallization at high densities [127], but with the addition of an infinitesimally thin barrier of arbitrary height u_h. Such a model was first introduced [90, 92] in the case of infinitely high barrier, to mimic the irreversible bond formation and study the effect of hopping in attractive glasses. An unambiguous advantage of the model is that thermodynamic and static properties of the system are strictly the same, either in the presence or in the absence of the barrier, because of its zero measure in phase space. However, the height of the barrier does have an effect on the dynamics, by setting the timescale of barrier crossing via the ratio $k_B T/u_h$. The equilibrium states being the same

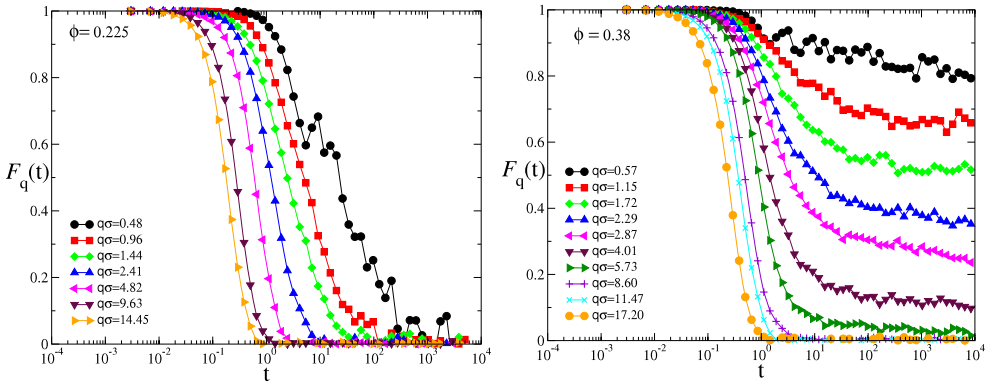

Figure 7. Wavevector dependence of density correlation functions $F_q(t)$ for chemical gelation at two fixed values of ϕ: just below percolation (left) and well within percolation (right). $\phi_p = 0.23$ for this model. Data taken from [91].

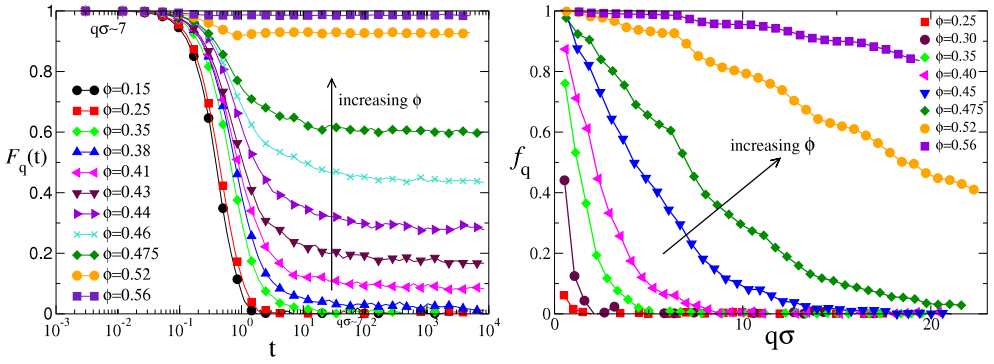

Figure 8. ϕ-dependence of $F_q(t)$ at the nearest-neighbour peak (left) and of the non-ergodicity parameter f_q (right) for chemical gelation. Data taken from [91].

with and without the barrier, the system can be readily equilibrated without the barrier, and then dynamics followed with the barrier, averaging over several initial configurations [91]. MD simulations of this system confirmed the results of Del Gado *et al* [41], but also allowed for a careful study of the wavevector dependence of the density correlators. Saika-Voivod *et al* showed that, in the case of infinite barrier height, the percolation transition generates a breaking of ergodicity for the system only at $q \to 0$, supporting the view that gelation in attractive systems corresponds to the formation of a network of infinite connectivity length [12]. Indeed, the cluster spanning the system at the transition is still very tenuous and almost massless (strictly so in the thermodynamic limit), so that it provides a non-ergodic confinement only at infinite length scale. Beyond the percolation transition, since the percolating cluster size P_∞ grows rapidly (as $(p - p_c)^\beta$), the non-ergodic behaviour also extends up to much larger q, until all particles are in the largest cluster and the system becomes highly non-ergodic.

To elucidate this important point, that will be frequently invoked in the rest of the review, we provide in figure 7 and 8 a representation of non-ergodic properties as ϕ increases in the case of infinite barrier height. In the studied system, the percolation threshold is estimated as $\phi_p \simeq 0.23$. For $\phi < \phi_p$ (left panel in figure 7), all studied density correlators $F_q(t)$ for various wavevectors, ranging from the smallest available compatibly with the simulated box

size ($q\sigma \approx 0.5$) to a large one where the decay is very fast ($q\sigma \approx 14.5$), decay to zero. However, for $\phi > \phi_p$ (right panel), a plateau emerges. The observed plateau, and hence the non-ergodicity parameter f_q, is found, at fixed ϕ, to strongly depend on q. Most importantly, with varying ϕ above the percolation threshold, larger q-values are ergodic while small ones are not. Starting from the smallest calculated q-value, which is found to become non-ergodic just slightly above percolation (within numerical accuracy), the system further becomes non-ergodic at larger and larger q-values as ϕ increases. Figure 8 shows the ϕ-dependence at a fixed wavevector corresponding to the static structure factor first peak $q\sigma \approx 7$ (left panel), where a detectable non-ergodic behaviour only occurs much beyond percolation for $\phi \gtrsim 0.35$. Also, the behaviour of f_q with increasing ϕ (right panel) suggests a crossover from a low-q signal, detecting the non-ergodic behaviour of just the percolating network, to a non-ergodic behaviour at all q, with a signature that is similar to that of glasses at large ϕ. We further note that, at percolation, f_q seems to become finite in a continuous way, starting from values close to zero (within numerical accuracy), as opposed to the case of glasses, where a discontinuous transition, also at the essence of MCT, is found. It is to be noted that the α-relaxation time at infinite barrier height diverges for each wavevector at a different packing fraction, coinciding with the percolation one only at the lowest studied q-values. Upon increasing q, the divergence happens when first the $F_q(t)$ shows a finite plateau. Thus, non-ergodicity is entirely governed by percolation in the permanent bond case.

As soon as the bond lifetime decreases, the system at first follows the percolation regime, as long as τ_B is longer than τ_α, and then crosses over to a standard glassy regime in full agreement with the lattice model findings of Del Gado *et al* [41, 91]. Approaching the glass transition, all wavevectors become simultaneously non-ergodic within numerical resolution. An important aspect of this study is that, by rescaling time taking into account the different bond lifetimes, all curves superimpose onto a master curve. This indicates that τ_B only affects the microscopic timescale, after which, when enough time has been waited to allow bond-breaking processes, the long-time behaviour (in particular f_q) is independent of the microscopic dynamics.

4. Routes to colloidal gelation

4.1. (Non-equilibrium) gelation as arrested phase separation

After discussing the high-density behaviour in section 2.8, we now focus on the low-density region of the phase diagram in short-ranged attractive colloids. As anticipated in figure 6, a natural interpretation coming out of MCT results [114, 128] and supported by a suitable comparison with experimental results [142], seemed to corroborate the thesis that a 'gel' phase observed in colloid–polymer mixtures is due to a kinetic arrest created by the bonds, and hence it would be just a natural extension—*in equilibrium*—of the attractive glass to much lower densities.

Before discussing in detail the dynamical behaviour of short-ranged attractive colloids, it is necessary to emphasize some important thermodynamic features of this type of systems. The range of attraction being extremely short, down to a few per cent of the particle diameter, the topology of the equilibrium phase diagram is different from that of standard atomic liquids. In particular, the gas–liquid phase separation is metastable with respect to the gas–crystal transition [143–145]. Despite being metastable, the intrinsic polydispersity of the particles helps in suppressing crystallization, and fluid properties inside the metastable region can be studied. A remarkable property of short-ranged attractive colloids (with interaction range smaller than a few per cent of the particle diameter) is the invariance of thermodynamic

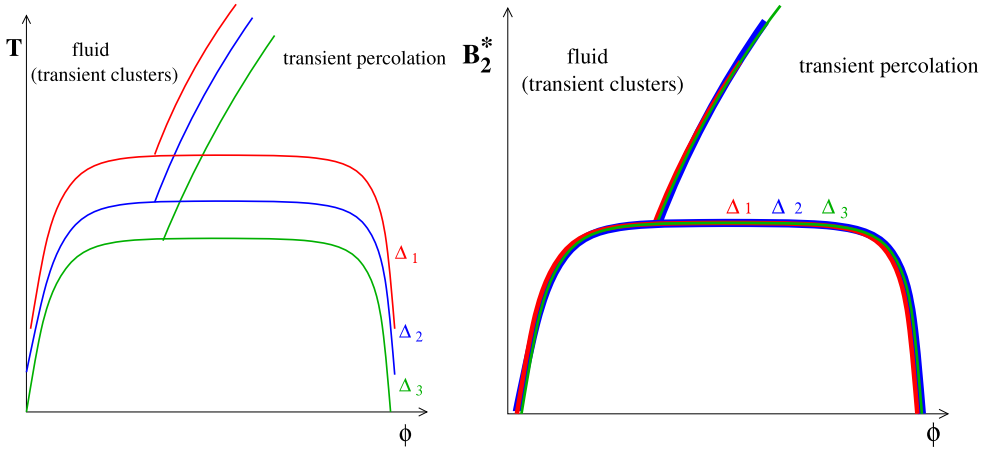

Figure 9. Representation of the Noro–Frenkel extended law of corresponding states for the phase diagram and (transient) percolation line of short-ranged attractive colloids. Here $\Delta_3 < \Delta_2 < \Delta_1 \lesssim 0.10\sigma$.

properties with respect to the specific potential shape and to the attractive range Δ when the normalized second virial coefficient $B_2^* \equiv B_2/B_2^{\mathrm{HS}}$ is used as control parameter. Here $B_2^{\mathrm{HS}} = 2\pi\sigma^3/3$ is the second virial coefficient for hard spheres. This invariance is known as the Noro–Frenkel extended law of corresponding states [146–148]. It implies that, if we plot the phase coexistence line in the (ϕ, B_2^*) plane for any short-ranged attractive potential of arbitrary shape and range within a few per cent of the particle diameter, all curves superimpose onto each other, as sketched in figure 9. Moreover, at fixed B_2^*, all thermodynamic properties such as $S(q)$ are identical for different shapes of short-ranged attractive models with small Δ. Also, the well known Baxter potential (the limit of the SW potential for infinitesimal width and infinite depth in such a way that B_2 is finite) [149] scales in the same way. Hence, the phase diagram of all of these systems can be represented by the phase diagram of the Baxter model, which has been carefully evaluated via grand-canonical Monte Carlo techniques by Miller and Frenkel [150, 151].

Numerical simulations for the 3%-width SW model [23] focused on the dynamics also at low ϕ. This study reported iso-diffusivity lines, i.e. lines where the normalized diffusion coefficient $DT^{-1/2}$ is constant, in the whole phase diagram, and showed that no sign of dynamical arrest was present for the system above the two-phase region at low ϕ, as shown in the phase diagram of figure 10. The same study showed that quenches inside the spinodal region generate a phase separation into a gas and an arrested dense phase. Indeed, $S(q)$ is initially found to follow the typical coarsening pattern: a growing low-q peak and a peak position moving towards lower and lower q-values with time. At some point, the coarsening process stops within the observation time-window and the structure does not evolve any further. This scenario of an arrested phase separation was observed if the quench was performed at a temperature below the intersection $T_{\mathrm{g}}^{\mathrm{sp}}$ between the spinodal and the extrapolated glass line, also shown in figure 10. Hence the origin of arrest can be traced back to an attractive glass transition of the denser phase. On the other hand, if the quench is limited to $T > T_{\mathrm{g}}^{\mathrm{sp}}$, the system would undergo a standard phase separation into a gas and a liquid phase [23, 152].

Many previous studies of quenches inside the phase-separating region in connection to gelation, or more generally to dynamical arrest, had been performed, both experimentally [44, 153], especially in the sticky (DLCA-like) limit, and in simulations [154–156]. However,

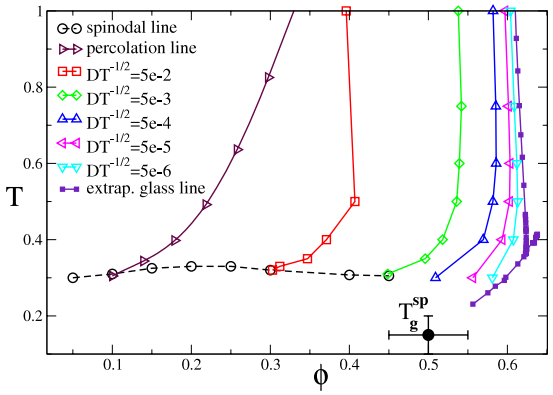

Figure 10. Phase diagram from simulations of a 3% SW binary mixture, reporting percolation, spinodal, iso-diffusivity and extrapolated glass lines. The latter is calculated through a mapping of the MCT glass lines onto the points where the diffusivity is found to diverge as a power-law [133]. It is found to only meet the spinodal at T_g^{sp} on the high-density side, indicating the absence of an equilibrium gel phase. Data taken from [23].

the relation of the thermodynamic line with the glass line was not clear. For the 3% SW case, a careful mapping [133] between the simulation data and MCT allows us to have a robust estimate of the glass line location, and hence to establish firmly for this model that arrest at low density can only result, via a non-equilibrium route, from an 'arrested (or interrupted) phase separation' process, since the attractive glass line crosses the spinodal line on the right-hand side of the critical point [23].

To investigate the question of whether the dependence on the width of the attractive potential could affect this picture, and allow for the existence of an equilibrium gel state above the coexistence curve, Foffi *et al* studied the dependence of dynamics on the attraction range for a SW binary mixture, down to the Baxter limit. Reference [24] showed that the well-width dependence of the dynamics is also controlled by B_2^*. Comparing the self-diffusion coefficient and the bond relaxation time at the same B_2^* values, universal scaling curves were found. Hence, within this picture, no equilibrium gel can exist above the spinodal region. This study suggests that the Noro–Frenkel scaling of thermodynamic properties can be pushed forward to invoke also a scaling of dynamical properties for short-ranged attractive colloids, up to the studied $\phi = 0.40$. However, this is a point deserving further investigation, since (i) a rescaling with B_2^* of the MCT glass lines themselves for different well widths does not hold [114, 107] and (ii) the study in [24] was limited to $\phi \leqslant 0.40$, whereas for larger packing fraction values many-body terms could become important and alter (but only at high ϕ) the simple B_2^* scaling. Subsequent work by the same authors focused on quenches inside the phase separation region for the extremely narrow case of the 0.5% SW model [157]. This work confirmed the arrested phase separation route for a quench below T_g^{sp}, reinforced by a comparison between molecular and Brownian dynamics. Again, a percolating network (generated during the phase separation process) is necessary for providing elasticity to the final structure. At too low ϕ the system forms compact clusters which continue to coarsen. These objects share some similarities with the so-called 'sticky gel beads' discussed within cluster MCT (CMCT) [158] and observed in experiments of salt-rich solutions of lysozyme [159].

Cates *et al* [68] proposed a framework for interpreting possible quench paths inside the binodal/spinodal region for short-ranged attractive colloids (see figure 2 in [68]). They suggest the possibility of two different routes to gel formation, according to the rate of the quench.

Their first route, which coincides with what we have called above arrested phase separation, is active when the system is quenched slowly and phase separation has time to develop. Hence, arrest is observed if the quench is below T_g^{sp} and if a percolating structure of the dense phase is generated. If the average density is such that phase separation does not produce a percolating structure, the system will form sticky beads, i.e. unconnected pieces of an attractive glass. Glass beads are expected to be internally frozen, because of the extremely low bond-breaking probability, but also freely diffusing in suspension. In practice, beads are prevented from forming a unique aggregate by the extremely long timescales involved in further coarsening. The second type of quench will be discussed below in the framework of CMCT.

We also mention recent numerical studies of a SW system undergoing a Brownian cluster dynamics [160], in which bonds are rigid, contrary to the standard algorithms to treat a SW interaction. In this work, a phase separation was found to arise prior to any slowing down of the dynamics in agreement with previous SW studies. Similar results were also obtained for a lattice model for T-shaped molecules in 2D, where gelation was also interpreted as the continuation of the glass line into the two-phase region [161].

The phase diagram depicted in figure 3 summarizes the results of numerical studies of a spherical short-ranged attractive potential (hard core plus attraction). Note that (i) no dynamic arrest takes place above the spinodal; (ii) dynamic arrest is observed for quenches below T_g^{sp}, inside the spinodal region. We further note that such an arrested phase separation scheme also applies to the case of longer-range attractive potential. Studies of a Lennard-Jones potential [162, 163] and of a larger (15%) SW model [164], for which the Noro–Frenkel mapping does not apply, have also reported that the glass line meets the two-phase region on the right-hand side of the critical point.

These simulation results are at odds with attempts to interpret colloidal gelation based on the ideal MCT predictions for short-ranged attractive potentials. For all potential shapes—including the SW model, hard-core attractive Yukawa and AO model—MCT predicts that the attractive glass line continues down to very low ϕ, passing above the coexistence region, and merging into the spinodal on the left hand-side of the critical point [114, 128]. These theoretical results (which do not account for the known difficulty, intrinsic in MCT, of predicting the exact location of T and ϕ of the glass line) predict the possibility that a stable 'equilibrium gel' at low ϕ exists, without an intervening phase separation. When dealing with MCT predictions, we have to take into account the fact that MCT always over-stabilizes the tendency to glassify. For HS, MCT underestimates the location of the arrest line by about 10%. In the case of attractive glasses (and consistently with the case of simple atomic potentials), the theory overestimates the arrest temperature by more than a factor of two. Moreover, at low ϕ, the interplay of dynamic arrest with phase separation and critical fluctuations is not correctly described by MCT, which is based on the assumption of a homogeneous fluid undergoing a glass transition. Once the theoretical MCT curves are properly mapped (using for example a bilinear transformation [132, 133]), the MCT attractive glass line is seen to intersect the spinodal line on the high-density branch, as shown in figure 10, suggesting that a proper treatment of the theoretical curves is consistent with the idea that arrest at low ϕ cannot be approached in equilibrium.

The attempt to fit MCT attractive glass line predictions with experimental data of a gel phase was carried out by Bergenholtz *et al* [142] for colloid–polymer mixtures of size ratio $\sim$0.08. While the agreement at large ϕ was reasonable, it was noted by the same authors that at low ϕ the theory seemed to 'insist on associating its predictions to observed equilibrium boundaries, rather than to transient gelation'. This seems to be a confirmation of the fact that the gel states are only observed within the binodal/spinodal region, although no sufficient characterization of the samples in terms of gravity effects and residual charges was done in

those early experiments. However, the same authors still point out the possibility that MCT could be more predictive for even shorter attraction ranges, where the gel line was expected to become more stable with respect to the binodal line. This possibility was supported by experimental works in the group of Zukoski [165, 166]. Indeed, they reported a homogeneous gel formation (that we would associate with an equilibrium route according to our classification of section 2) in semi-quantitative agreement with the corresponding MCT glass line for the very small size ratio 0.03. Static scattering experiments at low q on approaching the gel line and an investigation of the residual charge in such colloidal suspensions could be important to firmly establish whether these systems are indeed equilibrium gels and if they belong to the class of uncharged short-range attractive systems.

An attempt to improve the predictability of MCT at low ϕ was carried out by Kroy *et al*, in a generalization of the theory to consider the effect of cluster formation in the so-called cluster MCT (CMCT) [158]. This approach was carried out to combine aspects of standard MCT with irreversible aggregation of particles, embedding the inhomogeneous character arising from cluster formation into the homogeneous MCT approach. An ad hoc renormalization procedure is adopted, based on the following assumptions: (i) clusters cannot internally rearrange (although bond between clusters can be broken and re-formed); (ii) the interplay with phase separation is neglected (supposedly because the timescale of coarsening should be much longer than that of cluster aggregation). CMCT predicts an MCT-like glass transition of clusters, that is proposed to be the mechanism at hand when rapid quenches are performed inside the two-phase region [158, 68]. In this scheme, the system experiences an initial irreversible aggregation into clusters which would then arrest (double-ergodicity breaking), in a way that does not really distinguish whether the glass transition of clusters is due to jamming or to attractive bonds between them. No experimental evidence that CMCT actually captures the right physical ingredients has been reported since this, apart from the work of Sedgwick and coworkers [159]. In our opinion, in the purely short-range attractive case, the assumption of neglecting the phase separation with respect to irreversible cluster aggregation seems just too severe to be applied, and indeed it is not confirmed by all simulation studies of uncharged colloids. We comment that the theory could be potentially relevant for charged colloids, where the additional long-range repulsions help in inhibiting the phase separation. Indeed, the first evidence of cluster formation in colloid–polymer mixtures evolving toward a cluster glass transition, due to cluster jamming, was reported by Segrè *et al* [167]. We will discuss this phenomenon in section 4.2, since it was later on established that in such a system the colloid–colloid interaction is affected by charges [17], sufficiently to alter the phase diagram and gelation mechanism.

Finally we come back to experimental results addressing the interplay between gelation and phase separation. Several works [168, 47, 42, 44, 43] reported a clear proximity of the gel boundary with respect to the coexistence line, as well as detection of gel-like structures inside the spinodal region, although no precise estimates of the relative positions of the arrest and spinodal loci were available. Very recent experiments by Manley *et al* in colloid–polymer mixtures with moderate size ratios support the arrested phase separation scenario [22]. The authors combined the experimental observations of the frozen density fluctuations with an ad hoc use of MCT, where the static structure factor was taken directly from the experiments in the glass-like regime. Although this is not an 'orthodox' way to use MCT, and some adjustments of the parameters into play were employed, they provided evidence of an ergodicity breaking of the system after initial spinodal decomposition. Therefore, this study seems to reconcile theory, simulations and experiments supporting the picture of arrest at low packing fraction in term of an interrupted spinodal decomposition for (spherically symmetric) attractive colloids.

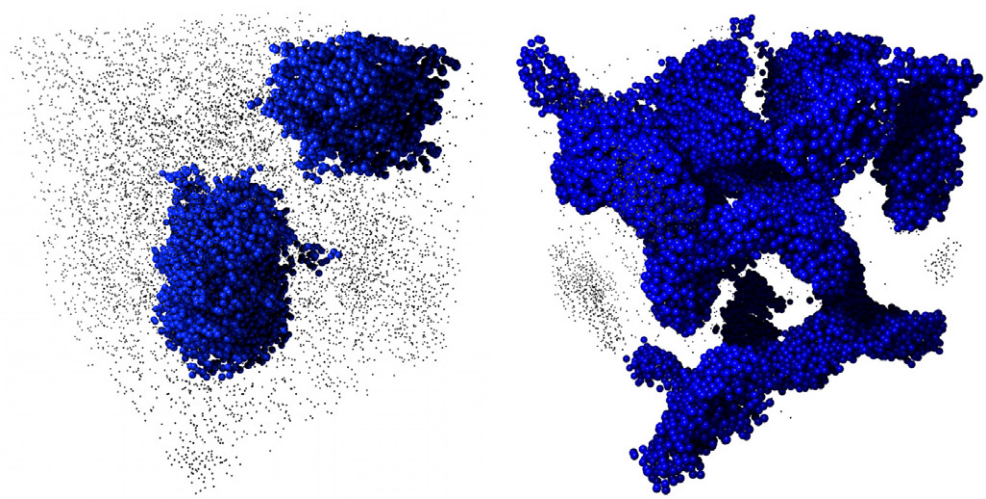

Figure 11. Reprinted with permission from [169]. Copyright 2006 by the American Physical Society. 3D reconstruction of clusters (left) and gel image (right) made of PMMA spheres with added polymers of size ratio 0.11: the compact structure of the clusters and the thick strands of the gel suggest that it results from an arrested phase separation after a not too deep quench. (For comparison, see figures 4 and 5 in [157] from simulations.)

In a subsequent study by the same group, Lu *et al* [169] reported advanced confocal microscopy experiments for different colloid–polymer size ratios and different ϕ in order to have a complete gel-transition phase diagram in the 3D plane involving attraction strength, packing fraction and size ratio (see figure 4 in [169]). For $\phi = 0.15$ and quite large size ratio $\approx$0.11–0.15, they observed, upon increasing added polymer concentration, a transition from a fluid of monomers to a gel, with an intermediate state that they call 'cluster phase'. The reconstructed 3D structures of the clusters and of the gel are shown in figure 11. The local density of the gel is rather large, while it shows, on larger length-scales, a fractal dimension of about 2.5, consistent with random aggregation. The almost bicontinuous thick pattern of the gel seems to indicate that it results from an arrested phase separation, although no explanation of the kinetics of gel formation is offered in the paper. The so-called clusters on the other hand are also rather compact spherical objects of many particles (about 1000), more indicative of an incomplete phase separation process (perhaps due to kinetic barriers) than of an equilibrium cluster phase. Indeed, such clusters seem to be rather frozen, and they do not exchange particles between them [169]. Moreover, the presence of residual monomers in suspension reinforces the idea of an initial phase separation scenario that is somehow interrupted. For shorter polymer additives, a similar type of clusters is also observed, although different in shape and structure: the fractal dimension decreases down to the DLCA value of about 1.7, and the clusters are not spherical at all but rather small (order of tens of particles) and chain-like.

This experiment raises a fundamental question in the study of colloid–polymer mixtures, namely the timescale of realistic systems as compared to the timescale accessed in simulations, especially when a simple effective one-component theoretical treatment is chosen for describing the colloid–colloid interactions. As underlined in a study regarding the re-entrant glass transition at high densities [170], the one-component effective picture is valid only strictly in the adiabatic limit, when polymers are truly mobile, due to the kinetic nature of the depletion interactions [171]. Increasing polymer concentration, polymers tend to approach their own overlap concentration, at which point (i) they will be highly non-ideal, (ii) they will not

be so mobile. To account for such non-ideal, non-adiabatic features in simulations is quite challenging, and some sort of multi-step coarse-graining (similar in spirit to that of [172]) could perhaps be investigated to be able to reach very large c_p close to the gelation threshold and should be the subject of future studies. Kinetic effects that polymers may have on the gelation processes and the role of entropic barriers associated with the different polymer configurations may emerge in an additional slowing down for further aggregation that stabilizes (at least on a very long timescale) smaller aggregates other than full phase separation and may create a gap between experiments and theory or simulations based on simple coarse-grained models. These effects could ultimately lead to an effective stabilization of bonds between particles, increasing formally the bond lifetime by more than a simple Arrhenius factor, and putting experiments in between MCT (dramatically over-estimating the bond stability at glass formation) and simulations of one-component effective models (Arrhenius bond lifetime dependence) [90, 91].

What is missing to definitely conclude that simple depletion attraction leads to an arrested state mediated by a phase-separation process is an independent accurate estimate of the position of the experimental gel with respect to the phase separation. Work is in progress to elucidate conclusively this aspect [173], building upon the Noro–Frenkel invariance of thermodynamics for short-range attractive potentials of arbitrary shape [146].

Finally, we mention a very recent experimental observation [67] of the interplay between phase separation and attractive glass transition in lysozyme solutions with added salt, i.e. in a short-ranged attractive protein solution. The addition of salt screens the protein–protein electrostatic repulsion and enhances the liquid–gas phase separation, so that a phase diagram of the same kind as that reported in figure 3 is found. Moreover, Cardinaux *et al* provide an estimate of the attractive glass boundary inside the spinodal region [67], through a set of careful centrifugation experiments. They show that, while proteins undergo a standard liquid–gas separation for $T > T_g^{sp}$, a coexistence of a denser glass and a gas is found below this threshold, in agreement with the results found in simulations of short-ranged attractive colloids [23, 157]. This experiment calls for further investigation inside the spinodal region, as well as for an extension of the effective protein–protein interaction model [174] in the regime where salt addition modifies the phase diagram.

4.2. Gels resulting from competition of attractive and repulsive interactions

The addition of a long-ranged repulsion to a short-ranged attraction is a way to act against phase separation, since $\gamma \leqslant 0$ (see section 2.4) [16, 175, 65]. In this case, particles prefer to aggregate in clusters of finite size, whose value depends on the particular thermodynamic conditions. Various experimental works reported the existence of an equilibrium cluster phase in charged (or weakly charged) colloid–polymer mixtures [167, 17, 93, 176, 18, 159, 177, 178], as well as in globular protein solutions at low ionic strength, such as lysozyme [93, 180, 181, 174]. This cluster phase arises from a delicate balance between short-range depletion (or hydrophobic or van der Waals for proteins) attraction and long-range screened electrostatic repulsion. Numerous numerical and theoretical works [21, 65, 182–184, 26, 185–191] proceeded in close connection with experiments.

A detailed numerical calculation of optimal cluster sizes, and related cluster shapes, by means of ground state energy calculations was performed by Mossa *et al* [65]. In this study, the short-ranged attraction was modelled for simplicity with a generalized Lennard-Jones potential [192], while the long-ranged repulsion was chosen as a Yukawa potential, to mimic screened electrostatic interactions. Therefore the total interaction potential is written as

$$V_{\text{total}}(r) = V_{SR}(r) + V_Y(r) = 4\epsilon\left[\left(\frac{\sigma}{r}\right)^{2\alpha} - \left(\frac{\sigma}{r}\right)^{\alpha}\right] + A\frac{e^{-r/\xi}}{r/\xi} \tag{2}$$

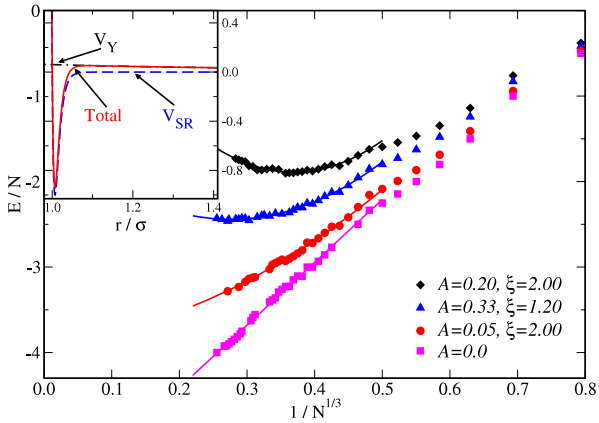

Figure 12. Reprinted with permission from [21]. Copyright 2004 by the American Physical Society. Ground state energy per particle E/N for clusters of size N for particles interacting via the total potential of equation (2), reported in the inset, upon variation of the repulsion parameters A and ξ. The $1/N^{1/3}$ behaviour is recovered in the absence of repulsion, while a minimum appears for larger and larger repulsions.

and it is shown in the inset of figure 12. Other studies involved closely related potentials, such as modifications of the DLVO potential [182, 183]. The ground state energy per particle E/N of a single cluster with varying size N was calculated for the potential in equation (2), through a basin-hopping algorithm [64, 65], and is reported in figure 12. In the absence of repulsion, i.e. for $A = 0$, the expected behaviour for large N, i.e. $E/N \propto N^{-1/3}$, is recovered, for various attraction widths ranging from Lennard-Jones to narrow wells [64, 65].

The addition of a long-range repulsion induces a minimum in the E/N versus N behaviour, signalling the emergence of an optimal cluster size N^*, whose value depends strongly on the parameters A and ξ. Hence, clusters with size greater than N^* are energetically disfavoured and, for $N \to \infty$, the system will prefer to fractionate into isolated clusters of size N^*, rather than undergo liquid condensation. In particular cases, i.e. when the condition $\gamma \simeq 0$ is realized, a clear minimum is not found, but the energy per particle displays a flat behaviour with increasing N [65], in which case the resulting cluster distribution will be highly polydisperse. Not only the optimal cluster size, but also the shape of the clusters, is found to be strongly parameter dependent. Indeed, clusters can be rather spherical or more elongated upon variation of the repulsion parameters [65]: while spherical structures are retained only when repulsion is rather weak and attraction is dominant, in general (quasi-) one-dimensional cluster growth is observed [18, 26, 188], in close analogy also with observations in protein gels [193–195, 55]. Such one-dimensional growth is not typically achieved by particles growing in strings, but rather in strands, in order to optimize locally the short-range attraction. In this respect, the ground state of the system is expected to be either a cluster crystal or a columnar phase at low density (depending again on the repulsive interaction parameters) [187, 188], or lamellar phase at larger densities [182, 188], in agreement with predictions for unscreened repulsive interactions [196–201], and with those of a mean-field model for Yukawa screened repulsion [185], as well as those of a stability fluctuation study [187]. Moreover, both the latter theoretical studies agree with the analytical calculation of the cluster energy in the limit $N \to \infty$ under the approximation of spherical, homogeneous clusters [65], that the control parameter γ, to discriminate between the presence of an equilibrium cluster phase and that of gas–liquid phase separation, is proportional to the product $A\xi^4$ for a repulsive Yukawa potential.

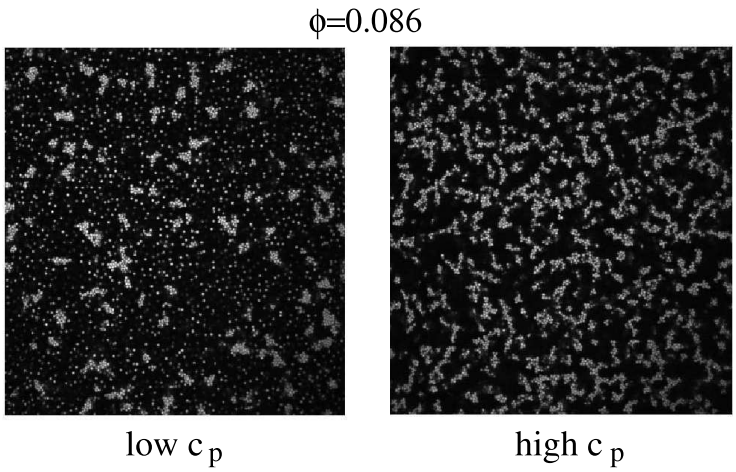

Figure 13. Reproduced from [176], with permission of IoP Publishing. Confocal microscopy images of charged PMMA particles in suspension with non-adsorbing polymers. In the left panel, a fluid cluster phase is observed, while a frozen gel network is found for increasing attraction strength in the right panel.

At finite T, entropic contributions will cause the cluster distribution to be polydisperse in size, with a growing number of clusters of the optimal size as attraction gets stronger, giving rise to a marked peak in cluster distribution [21]. However, due to the fact that the arrangement into clusters is driven by strictly energetic balance, they are dominating structures at low enough T. Hence, clusters, not particles, can act as building blocks of a dynamically arrested state. Several confocal microscopy experiments have revealed the presence of the clusters leading, with increasing ϕ, to an arrested state. We report in figure 13 one of these experiments taken from Sedgwick *et al* [176], corresponding to charged density-matched PMMA spheres in solutions with non-adsorbing polymers, at two values of polymer concentration, respectively in the fluid cluster region (left panel) and in the frozen network region (right panel).

Before discussing the various aspects related to the arrest transition of clusters, let us focus on the signatures of a cluster phase in the static structure of the system. In the case of short-range attraction plus long-range repulsion, a dominant length scale deriving from the balance of attraction and repulsion [185, 187] modulates the structure into periodic patterns [182, 188]. This is a general feature of competing interactions of any nature [89, 202, 180]. In the static structure factor, a cluster pre-peak at a finite length appears, clearly a distinctive feature from the typical increase found in purely attractive systems. A number of experimental works have reported this feature. Firstly, the slightly charged PMMA spheres with added polymers studied by Segrè *et al* [167], reported the observation of a colloidal equilibrium cluster phase at low density, although the role of charges was not fully recognized in their original work. As the authors state in their manuscript, a peak in $S(q)$ is observed at low q even at very low ϕ, where the system does not form a gel but remains ergodic. Indeed, it is important to note that the existence of the pre-peak directly derives from the interaction potential, hence it is a feature that is present both in the fluid and in the gel phase. More specifically, it is found in the ergodic cluster phase as well as in the presence of a percolating network.

More recently, emphasis on the cluster phase and on the cluster peak signature in $S(q)$ has been put forward by Stradner *et al* [93] in solutions of lysozyme under low-salt conditions, as well as again in short-ranged attractive charged PMMA spheres. For lysozyme solutions,

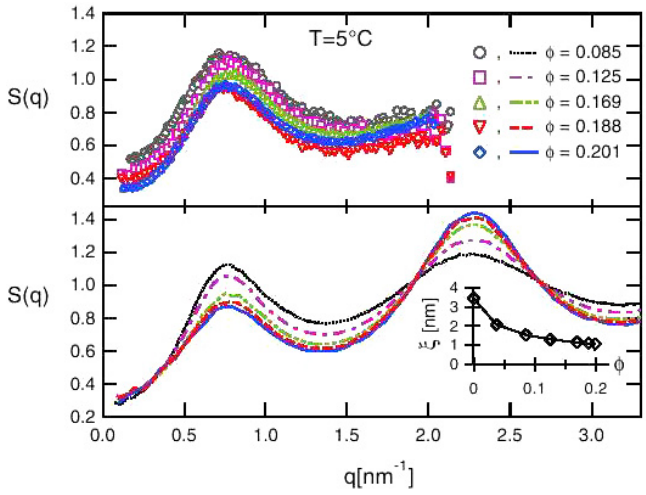

Figure 14. Static structure factor from SAXS measurements (top) and simulations (bottom) for salt-free solutions of lysozyme at various studied ϕ and $T = 5\,^{\circ}\mathrm{C}$. A typical cluster–cluster peak, whose position remains constant in ϕ, is visible. Inset: the variation of the screening length ξ in nm (the lysozyme molecule is treated as a sphere of diameter 3.4 nm). Reproduced from [174].

a remarkable invariance of the cluster peak position q_c^* was reported with ϕ. Numerical simulations [174] of a total interaction potential, of the form described by equation (2), have shown that a simple effective model based on competing interactions can indeed be successful in describing the clustering phenomenon, even for lysozyme solutions. A comparison of $S(q)$ in simulations and experiments, for zero-salt lysozyme solutions, is provided in figure 14 for various studied protein packing fractions. Importantly, the long-range repulsive part of the total potential is fixed by experimental conditions, with the screening length varying with protein concentration as reported in the inset, while the attractive depth is chosen via a single-parameter fit to map experimental measurements. This choice is then kept fixed for all studied ϕ [174].

So far, we have established that systems with competing short-range attraction and long-range repulsion form equilibrium clusters and do not phase separate (at least for large enough ξ). Hence, upon increasing attraction strength, an arrest transition, mediated by the clusters, not by the particles themselves, occurs. The nature of the cluster arrest transition will depend on the residual 'effective' cluster–cluster interactions [21, 26]. To a first order approximation, assuming spherical clusters homogeneously packed and monodisperse in size, it is found that cluster–cluster interactions have the same screening length as the particle–particle interactions, with renormalized amplitude [21]. For large enough screening lengths, i.e. at least of the order of a particle diameter, repulsive interactions are dominant between clusters and may induce a repulsive Wigner glass transition at low density, preventing the formation of a Wigner crystal of clusters thanks to the intrinsic cluster polydispersity. Here, repulsion is the mechanism leading to the arrest and no percolating network is indeed detected in the simulations, although showing non-ergodic features [21]. The Wigner glass of clusters was observed in simulations, but also reinforced by MCT calculations based on the renormalized cluster–cluster interactions [21]. Moreover, MCT calculations for a double Yukawa potential (short-range attraction plus long-range repulsion) also support this scenario [184].

However, if the screening length is smaller, i.e. roughly of the order of a particle radius, cluster–cluster interactions are not so relevant and the short-range attraction for two particles

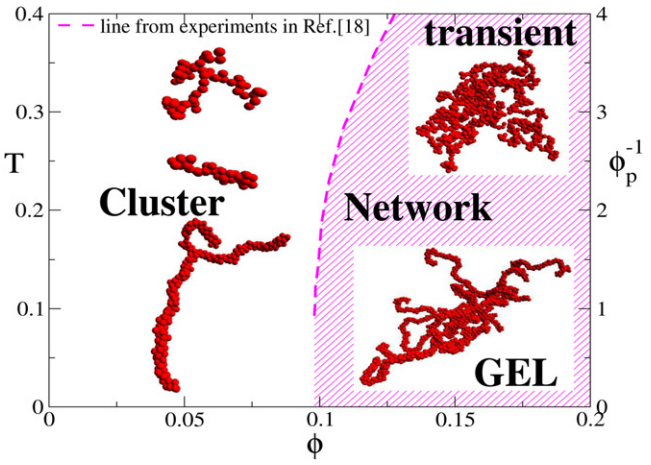

Figure 15. Phase diagram for charged PMMA spheres with non-adsorbing polymers from [18]. On the x-axis, colloid packing fraction ϕ is reported, while on the y-axis temperature (from simulations in [26]) and inverse added polymer packing fraction ϕ_p^{-1} are shown (left and right sides, respectively). The line, taken from the experimental work of [18], divides the region where a cluster phase is observed from that of network formation. Cluster and gel snapshots are taken from simulations in [26]. A transition in cluster shapes is shown from random transient clusters to long-lived spirals upon increasing attraction strength. The percolating region in simulations is in good agreement with that found in experiments, and a gelation transition of branching spirals is found.

at contact may act as a glue for the gel formation. In this second case, the gel formation can be identified with the percolation of the clusters [26, 183]. It is to be noticed that the difference between these two cases is very subtle, and strongly dependent on the details of the potential parameters, but the mechanism for arrest that results is very different: a 'glass' of repulsive clusters in one case and a branching mechanism of adjacent particles within clusters in the other. Moreover, different paths to achieve the low-temperature states, i.e. for example rapid quenches, can induce a so-called 'arrested micro-phase separation' [86], where clusters, despite repulsion being strong, remain trapped in a metastable percolating gel-like state for a long time, without equilibrating to the underlying Wigner glass or crystal, that would be achieved under a slow equilibration approach [21]. We finally comment that, also in the case of large screening lengths, a crossover from the Wigner glass behaviour to a percolating gel transition with increasing ϕ should be observed (as also suggested by figure 4). This crossover is currently under investigation. Interestingly, a Wigner glass of clusters has only been predicted by simulations, but no clear experimental observation has been provided yet, at least for simple spherical colloids.

The case of cluster branching into a gel network was reported in a confocal microscopy experiment of charged PMMA with added non-adsorbing polymers by Campbell *et al* [18]. These authors showed the emergence of an equilibrium cluster phase at low ϕ merging into a percolating network with increasing ϕ, with the observed phase diagram drawn in figure 15. In particular, they were able to identify the organization of clusters in a well defined geometry corresponding to the so-called Bernal spiral [203], i.e. a two-stranded spiral formed by face-sharing tetrahedra. A 2D reconstruction of a gel slab, with a highlight of the Bernal spiral structure, is found in figure 16 (left panel). Interestingly, ground-state cluster energy calculations had been already performed for parameters strikingly close to the experimental ones, i.e. $A \simeq 8$ and $\xi = 0.5$ in [65], predicting a Bernal spiral ground state (although the

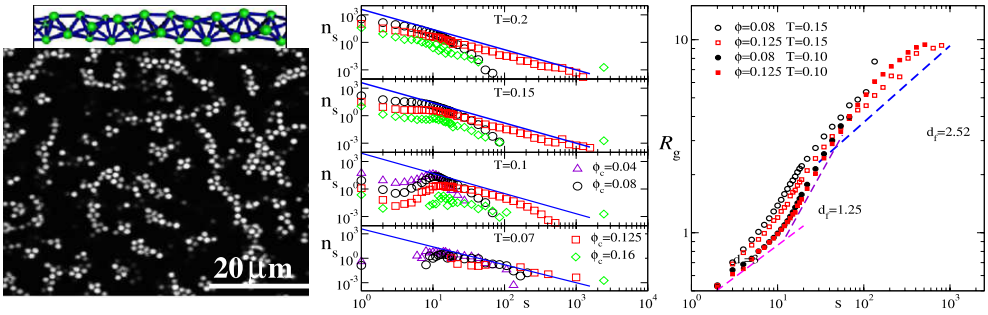

Figure 16. Left panel: reprinted with permission from [18]. Copyright 2005 by the American Physical Society. Confocal microscopy image of the network with spiral-like structure. The Bernal spiral structure is also drawn. Middle panel: cluster size distributions $n(s)$ with varying T and ϕ. Right panel: radius of gyration R_g at $\phi = 0.08$, i.e. below percolation, and $\phi = 0.125$, at percolation for high and low T: $T = 0.15$ and $T = 0.1$. Middle and left panels from simulations reproduced with permission from [26]. Copyright 2005 Am. Chem. Soc. Data show that at high T the formation of (transient) random clusters leads to (transient) random percolation, while at low T the organization of the system into the energetically preferred spirals provides quasi-one-dimensional growth of clusters, approaching a random percolation of spirals.

specific structure was not recognized), which with increasing size of the cluster can only grow linearly along one dimension.

Brownian dynamics simulations in bulk conditions were then carried out [26] with an effective potential aiming to to mimic precisely the experimental conditions of [18, 177]. Combined results from experiments and simulations are shown in figure 15. An aggregation into spiral clusters was detected as well as a branching of spiral clusters giving rise to non-ergodic behaviour. This is possible due to the fact that the residual repulsive interactions between spirals are negligible, while a branching point is a defect of the perfect spiral structure at low, but non-zero T, providing rigidity to the network. An interesting aspect pointed out by the simulations is that percolation is observed both at high and low temperatures, with an intermediate non-percolating region (re-entrant percolation). The cluster size distributions $n(s)$ for the studied state points are reported in figure 16 (middle panel). At high T, a typical transient percolation is found and no gel state is formed but only a transient network. In this case the fractal dimension of the clusters is consistent with random percolation. At intermediate temperatures, the system starts to organize itself into spirals to minimize the energy, hence a peak in the cluster distribution arises. While the system rescales its basic units from monomers to spirals (for which the minimal size is of order ∼10 particles), the effective packing fraction decreases, so that percolation ceases. A further decrease in T allows for percolation of spirals rather than particles, while monomers become absent. Interestingly, the spirals have an almost linear fractal dimension, i.e. $d_f \sim 1.25$, while at percolation the branching mechanism follows again the random universal exponent, i.e. a random percolation of spirals. This scenario is well described by the evolution of the radius of gyration $R_g \equiv 1/N[\sum_{i=1}^{N}(\mathbf{r}_i - \mathbf{R}_{CM})^2]^{1/2}$ reported in figure 16 (right panel) for two studied values of packing fractions $\phi = 0.08$ (below percolation) and $\phi = 0.125$ (at percolation) at high and low T. We further note that, at low T, the cluster structure is independent of ϕ for all sizes, suggesting the approach to the ground state structure. We can distinguish an initial spherical growth at small s compatible with a fractal dimension $d_f = 3$ [65], followed by an almost-linear growth, i.e. $d_f \sim 1.25$, in the size interval where long spirals are forming, $10 \lesssim s \lesssim 100$, and finally a recovery of the random organization of spirals for large s. Beyond this point, the high- and low-T results are almost coincident. More details can be found in [26].

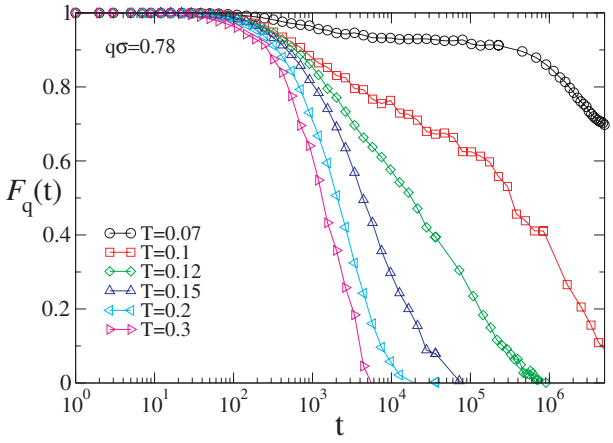

Figure 17. Density auto-correlation functions signalling non-ergodic behaviour of the branching gel of spirals at $\phi = 0.16$ and decreasing T. Note that at this ϕ all state points are within the percolating region, but only those at low T show an arrest transition. Reproduced with permission from [26]. Copyright 2005 Am. Chem. Soc.

It is important at this point to focus on the visualization of the clusters. These are reported together with the phase diagram in figure 15. A comparison of the percolating clusters observed at $\phi = 0.125$ respectively at high and low T in the network region is offered. For $T = 0.15$ a random structure, which is transient in time, is observed, mostly organized into single-lined chains. On the other hand, for $T = 0.07$, a branching mechanism of spiral strands has taken place to form a gel. Here, no single-line chains are observed, but the only defects in the spiral structures are the junction points allowing the establishment of a macroscopic network. In between these two behaviours, a shrinking of the largest cluster accompanied by a reorganization into spirals is observed due to the above-mentioned competition between entropic and energetic effects [26]. This can be visualized in the cluster side of the diagram, where the reorganization of small clusters at $\phi = 0.08$ for $T = 0.15, 0.1, 0.07$ is shown. An almost perfect spiral is recovered at the lowest T. The detailed spiral structure has also been confirmed by the study of the rotational invariant distributions directly compared to theoretical values and experimental curves [18, 26].

Being the cluster ground state structures, bonds will be less and less broken with decreasing T, and a gel state with a marked plateau in the MSD and density correlation functions is detected, as shown in figure 17. Here, only a partial investigation of the q-dependence of $F_q(t)$ was carried out at $\phi = 0.16$, suggesting however a non-ergodic behaviour for a gel structure only at the smallest studied q-values, in the region of the structure factor pre-peak, while smaller length-scales retain quasi-ergodicity, despite a marked slowing down of the dynamics also observed in the MSD [26]. The functional form of $F_q(t)$ is found to depend strongly on q and T. We note that, at this ϕ, the system always percolates for $T < 0.2$, but only at low T is an arrest transition found. Hence the random percolating clusters shown in figure 15 do not show any slow relaxation as anticipated before. In summary, we have reported a case of an equilibrium route to gelation, whose phase diagram belongs to the category of figure 4. However, in this special case, the small value of ξ is not sufficient to generate a Wigner glass. Interestingly, it also turns out that a total spherical potential of the kind of equation (2) is capable of producing peculiar self-assembled structures, providing in the case of the low-T Bernal spirals an effective particle coordination number strictly equal to six.

Similar results to those of [26] have been reported for a modification of the DLVO potential, for which de Candia *et al* also studied the organization into ordered columnar and lamellar phases at low T [188], pointing out that at low ϕ columns are expected, being more stable than the cluster crystal (due to the small screening length in the studied case), while at larger ϕ lamellae should be formed. However, this phase is never observed spontaneously during a simulation, due to the intervening of disordered gel phases of the kind discussed above.

The scenario of competing interactions and formation of a cluster phase is quite general and can be found in many examples. It was already established in other types of systems where competing interactions take place, such as in micelles [199, 204] and nanoparticles deposited at the air–water interface [205, 200]. Recently it was also discussed in other charged, neutral or magnetic colloidal systems. For example, in Laponite suspensions different arrested states are observed upon varying concentration or ionic strength [206–208]. It has been hypothesized that different mechanisms are responsible for arrest: a transition mediated by the clusters at low concentrations, followed by an arrested state mediated by particles at larger concentrations, which is still debated in nature [100, 209, 207, 208]. More recently, a similar behaviour was observed for other clay suspensions, such as sodium Cloisite [210], where a low-density solid was interpreted in terms of a Wigner glass of clusters at low ionic strength. Also, for charged liposomes in solutions with charged polyelectrolytes, large equilibrium clusters are observed, these being stabilized by charge complexation [211–214], while, in mixtures of star polymers and linear chains [215, 202], entropic effects give origin to a long-ranged repulsion and depletion effects induced by the linear chains induce a short-ranged attraction among the stars, which form small clusters. Also, clustering has been observed in water solutions of silver iodide [216] and molybdenum oxide [217], as well as paramagnetic colloids in 2D [218]. In protein solutions, clusters have been reported not only for lysozyme, but also for cytochrome c proteins [180], haemoglobins [219] and ferritins [220], thereby suggesting an underlying similarity of the competing interaction mechanism, which is applicable to both colloid and protein solutions. A case where cluster formation has a different origin, arising from purely repulsive interactions, is that of ultrasoft systems [221].

4.3. Patchy models

The formation of an equilibrium gel, and the exploration of the dynamics close to the ideal gel state, can also be achieved without the need to invoke additional forces such as long-range repulsion. Indeed, purely attractive interactions can be tuned to explore the case of small γ. To this aim, it is sufficient to ensure a low coordination number for aggregation, so that there is no driving force for the system to form a bulk liquid, while network formation is enhanced. In this framework, hence, $e_{\text{bulk}} \simeq e_{\text{surface}}$ and for $T \to 0$ the system will tend to form a disordered fully connected network. The concepts of limited-valency and of patchy particles (or as explained later of patchy-like particles) have been recently emerging as a new class of materials to build, among various issues, ideal colloidal gels.

Experimental realization of such systems is growing at fast pace, through sophisticated engineering of 'colloidal molecules' [3, 222–226], as well as use of relative interactions to design colloids with valency [227]. An example of experimental patchy colloids is shown in figure 18 (top), reproduced from [224]. The aim of these studies is, of course, not limited to gelation. Indeed, such particles offer the possibility to be used as building blocks of specifically designed self-assembled structures [228–234], having in mind the ambitious goal to realize a colloidal diamond crystal [3, 5, 235], which may offer the possibility of a large photonic band gap for many industrial and technical purposes [236, 237]. Moreover, the implications of patchy colloids for proteins [238], which are patchy by nature, could be significant. Literature on this

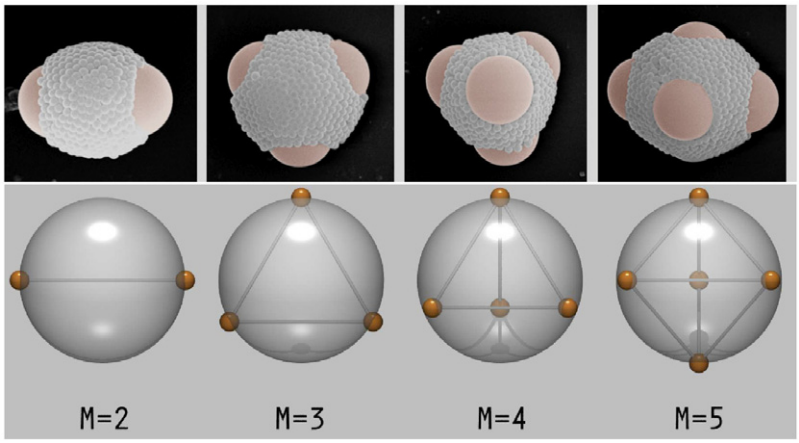

Figure 18. Top: adapted with permission from [224]. Copyright 2005: American Chemical Society. Experimental particles realized from bidisperse colloids in water droplets. Courtesy of G-R Yi. Bottom: reprinted with permission from [27]. Copyright 2006 by the American Physical Society. Primitive models of patchy particles used in the theoretical study of [27].

extremely new and emerging topic is growing fast, due to the many possibilities offered by the realization of new colloidal molecules [5]. Numerical studies are being used to design specific self-assembly [229–234], as well as to determine optimized circularly (spherically) symmetric interactions in 2D (3D) for producing targeted self-assembly with low coordination numbers: by inverse methods, square and honeycomb lattices [239, 240] have been assembled in 2D, and a cubic lattice in 3D [241]. In this paragraph, we will only focus on the knowledge about phase diagram and gelation of patchy colloids that is being recently established.

Models have started to appear in the literature, taking into account not only a spherical attraction, but also angular constraints for bond formation [242]. Similar ideas have been exploited in the study of protein phase diagrams [243, 244]. However, these earlier works have not addressed the important question of how to systematically affect the phase diagram of attractive colloids in order to prevent phase separation and allow ideal gel formation. To this end, we recently revisited [28, 245] a family of limited-valency models introduced by Speedy and Debenedetti [246, 247], where particles interact via a simple square well potential, but only with a pre-defined maximum number of attractive nearest neighbours, $N_{\max}$, while hard-core interactions are present for additional neighbours. This model can be viewed as a toy model for particles with randomly located sticky spots, due to the absence of any angular constraint. Moreover, the sticky spots are not fixed, but can roll onto the particle surface, also relatively to each other. The disadvantage of such model is that the Hamiltonian contains a many-body term, taking into account how many bonded neighbours are present for each particle at any given time. Notwithstanding this, the model is the simplest generalization of attractive spherical models, and its study can be built on the vast knowledge of the phase diagram and dynamics for a simple SW potential.

The addition of the $N_{\max}$ constraint effectively reduces the tendency of the system to phase separate, when $N_{\max}$ is fewer than six neighbours. In figure 19 (left), the liquid–gas spinodal and percolation lines are drawn for $N_{\max} = 3, 4, 5$ and for the standard SW, where by geometric constraints $N_{\max} = 12$. Not only the temperature or energy scale where phase separation takes place decreases with decreasing $N_{\max}$, as also previously observed with increasing angular constraints [242], but most importantly a significant shift in the critical packing fraction, is

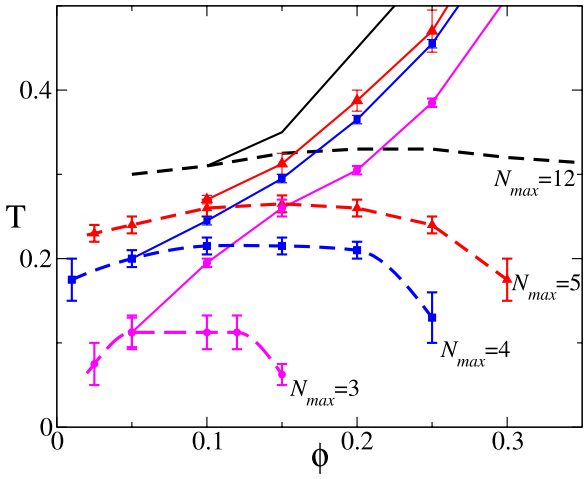

Figure 19. Reprinted with permission from [28]. Copyright 2005 by the American Physical Society. Phase diagram variation with $N_{\max}$: the phase-separating region is pushed to lower temperatures, but most importantly to lower and lower densities. A similar fate is found for the transient percolation lines.

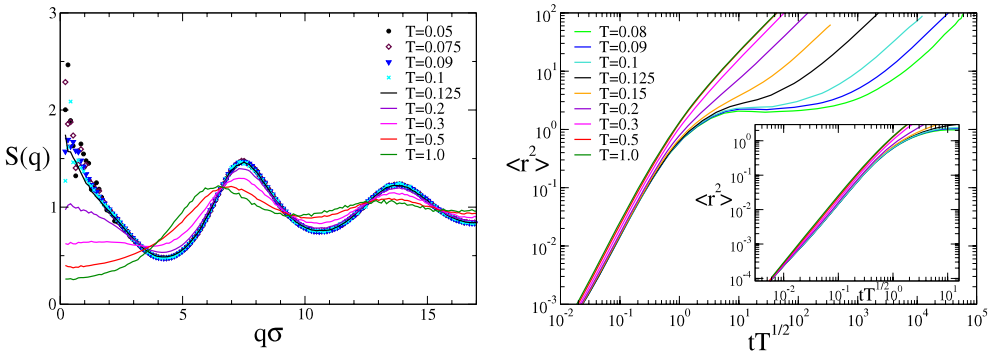

Figure 20. $S(q)$ and MSD for $N_{\max} = 3$ and $\phi = 0.20$ at different T. Below $T \lesssim 0.1$ the structure does not evolve further and the system displays an equilibrium gel transition. The MSD data are plotted as a function of $tT^{1/2}$ to take into account the difference in thermal velocities. Data taken from [245, 28].

observed. The shift of the coexistence region is accompanied by that of the transient percolation line. Hence, a wide region emerges at low densities, where the system can be equilibrated down to very low T without an intervening phase separation. In this region, for example at fixed ϕ upon lowering T (e.g. $\phi = 0.20$ for $N_{\max} = 3$ or $\phi = 0.30$ for $N_{\max} = 4$), the bond lifetime grows by orders of magnitude with respect to the unconstrained SW case [28], allowing for the persistence in time of the percolating network, since the system is already well within the percolating region. Therefore, gelation can be approached in equilibrium.

Let us focus on the properties of this low-ϕ equilibrium gel state. We show in figure 20 the evolution of $S(q)$ (left) and of the MSD (right) for various studied temperatures at $\phi = 0.20$ and $N_{\max} = 3$. The static structure factor displays progressive structuring of peaks at $q \sim 2\pi/\sigma$ and multiples thereof as T decreases. Most importantly, an increase of the low-q signal is detected, which saturates to a finite value. Indeed, around $T \sim 0.1$, the system has already formed about

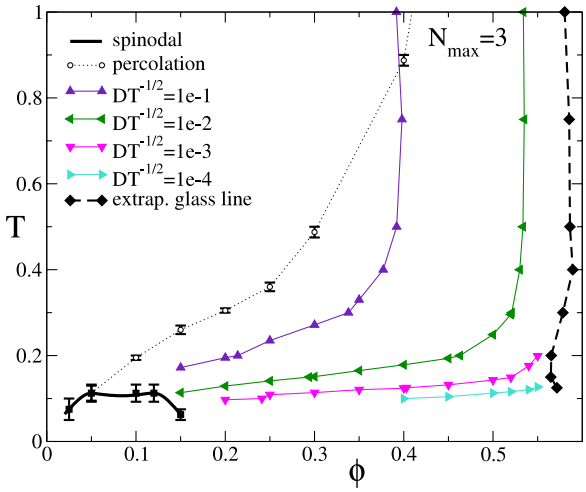

Figure 21. Adapted with permission from [245]. Copyright 2006, American Institute of Physics. Extended phase diagram and iso-diffusivity lines for $N_{\max} = 3$.

99% of the possible bonds, so that no further restructuring is allowed, and indeed $S(q)$ remains constant for lower T. The increase at low q is an echo of the nearby phase separation, and indicates that the system is highly compressible due to the large voids separating the network branches. Hence, large inhomogeneities are indicative of the equilibrium gel structure.

The MSD, shown in figure 20 (right), displays with decreasing T a clear plateau, i.e. a significant slowing down of the dynamics. Such a plateau arises at a very large length scale, of the order of σ, suggestive of the large localization length that is due to the large voids between the network branches. Indeed, the localization length was found to depend sensitively on ϕ, but not on T. It is highlighted in the inset that not only does the long-time plateau display a marked T-dependence, but also a short–intermediate-time behaviour shows difference for the different studied T. This is due to caging within the attractive well, and indeed appears for $\langle r^2 \rangle \sim \Delta^2$, compatibly with the bond distance.

Also, the density correlators display marked plateaus [28] at small q-values, from which it was possible to establish that (i) the arrest transition shows a marked q-dependence in contrast to what is found in standard glasses and (ii) the non-ergodicity parameter f_q appears to grow continuously from zero (within numerical accuracy) and displays a finite signal only at very small q, much smaller than the typical nearest-neighbour distance. Importantly, at all studied T where it was possible to equilibrate, i.e. $T > 0.05$, the system after a long time recovers ergodicity. For lower T, the bond lifetime becomes longer than the observation time. Hence, exactly what we defined as an equilibrium gel applies here, a disordered state, approached through successive equilibrium states, with a 'long' relaxation time. Ideally, if the observation time was infinite, the ideal gel at $T = 0$ would be accessed. However, we notice that at fixed ϕ, while T is so low that the system has reached the (almost) fully connected state (i.e. $T \lesssim 0.1$), the properties of the gel, i.e. localization length, $S(q)$, f_q, do not show further dependence on T, hence the ideal gel is just a continuation of the equilibrium gel to longer and longer bond lifetime and slower and slower relaxation.

The study of the dynamical behaviour in the (ϕ, T) plane, combined with the phase diagram, is reported in figure 21 for $N_{\max} = 3$, revealing that there are two distinct arrest transition mechanisms [245]. Indeed, the iso-diffusivity curves, covering a slowing down

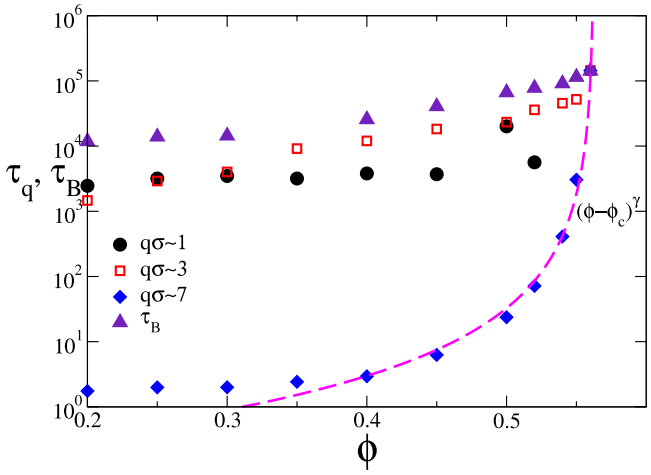

Figure 22. Adapted with permission from [245]. Copyright 2006, American Institute of Physics. Bond lifetime and relaxation times at different wavevectors as a function of ϕ for fixed low $T = 0.1$ and $N_{\max} = 3$. While low-q dynamics is slaved to the bond lifetime, indicating the gel nature of the arrest, the large-q dynamics is completely decoupled and only becomes slow at the glass transition with a power-law behaviour. Here the exponent γ is ≈2.5.

of four orders of magnitude, show a clear vertical shape at high ϕ turning into a rather flat horizontal shape at low T. For large ϕ, arrest is governed by the hard core only. Indeed, the diffusion coefficient follows, along isotherms, a power law as $(\phi_c - \phi)^\gamma$, where the extrapolated glass transition values $\phi_c(T)$ do not show signification variation with T and remain always close to the hard-sphere characteristic glass value (≈0.58). For smaller ϕ and low T, the iso-diffusivity lines cross from vertical to horizontal, meeting the spinodal region with an almost flat slope. This horizontal region is where the system forms an almost perfect network, with $\gtrsim$99% of the particles having saturated the $N_{\max}$ available bonds, but with a high degree of disorder, signalled by a finite configurational entropy [248, 249]. Dynamics becomes increasingly slow and an equilibrium gel is formed. In this region, D follows a purely Arrhenius dependence on T, suggesting that the activation barrier to break bonds is the key quantity controlling the dynamics.

To elucidate better this argument, we show in figure 22 the ϕ-dependence of the bond lifetime τ_B and of the relaxation timescale τ_q at three different q-values for fixed $T = 0.1$. It is clear that, at all ϕ, the bond lifetime is the slowest timescale of the system, governing entirely the dynamics at this low T. Moreover, the low q dynamics is ruled by τ_B, τ_q being proportional to τ_B in this region, but the large-q relaxation is completely decoupled at low ϕ. Indeed, it follows a typical (glassy) power-law increase and joins τ_B at large ϕ. Note that large q here indicates the typical nearest-neighbour distance, i.e. the relevant length-scale for a glass transition. Indeed, looking at the full decay of density auto-correlation functions, we observe that, in the gel phase, for $q\sigma \sim 7$ no slowing down is detected at all, while a clear plateau is observed for smaller q as reported in figure 23-left. These results raise the fundamental problem that only a certain q-window is appropriate for looking at gel dynamics. Therefore, with respect to glasses, experimental studies have to focus strictly in the low-q limit. The gel-to-glass transition is evident from the behaviour of the non-ergodicity parameter f_q with increasing ϕ, shown in figure 23 (right).

Hence, we clearly identify a crossover from gel to glass dynamics, that appears to be quite sudden in a small window of ϕ. It would be interesting to focus future studies on the

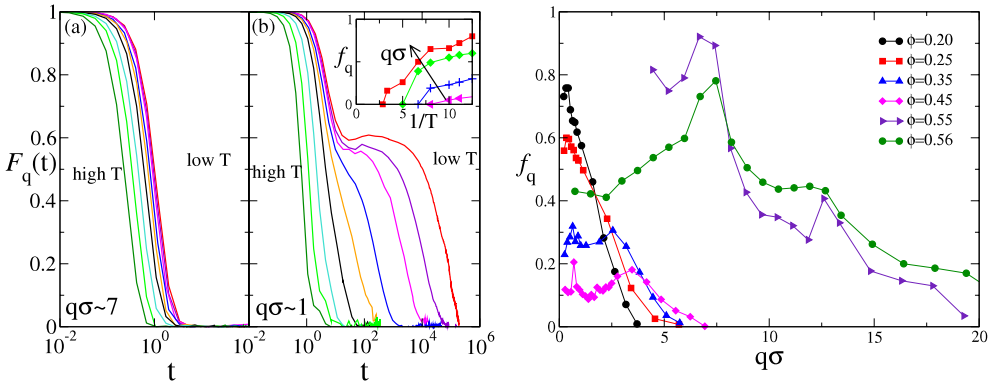

Figure 23. Left: $F_q(t)$ behaviour with T at $\phi = 0.20$ and $N_{max} = 3$. No slow relaxation is detected at the nearest-neighbour length scale (left). Inset: plateau value f_q as a function of $1/T$ for $q\sigma = 0.2, 1, 2, 3$ from top to bottom. Data from [28]. Right: adapted with permission from [245]. Copyright 2006, American Institute of Physics. Non-ergodicity parameter as a function of ϕ at $T = 0.1$ and $N_{max} = 3$.

investigation of this crossover, if it is smooth or discontinuous, given also the fact that evidence of a competition between the two transitions is found at intermediate ϕ, signalled by anomalous dynamics similar to that encountered in the SW potential between attractive and repulsive glasses, i.e. sub-diffusive MSD and logarithmic decay for the density correlation functions. Finally we remark that, in the N_{max} model, no evidence of an attractive glass is found, due probably to the low-coordination structure which forbids the formation of attractive cages at low T (here perhaps the study of even lower T would be appropriate, if feasible), as well as the fact that MCT would predict results similar to those for a standard SW, hence an attractive glass instead of a gel line [250].

Despite the simplicity of the N_{max} model, it allows us to establish distinct gel features with respect to standard glasses: (i) a very large localization length, much larger than that typical of glasses; (ii) non-ergodicity properties strongly dependent on the length-scale of observation; (iii) a static structure factor displaying a growing, but finite signal at low q. Interestingly, in agreement with previous studies of the bond lifetime influence of the dynamics discussed in section 3, the density autocorrelation functions start to display non-ergodic features, i.e. the emergence of a clear plateau, at first at very low q, then growing in q with further decreasing T. Thus, the gel transition temperature strongly depends on the wavelength of observation, as shown in the inset of figure 23, in contrast to what is commonly found in glasses, where all length-scales become non-ergodic simultaneously at a single, well defined T_g. Hence, if one looks at the typical nearest-neighbour distance, the dynamics appears completely ergodic, in analogy to what is observed in chemical gelation. Only with further increase of density or decrease of temperature do all length-scales successively become non-ergodic, crossing over to a glassy behaviour, in agreement with earlier models [41, 91] and with studies in polymer gel-to-glass transition [251].

From the N_{max} model, a step towards more realistic models with fixed, geometrically organized sticky spots, to mimic experimentally available particles [3], can be done using ideas already established in the physics of associating liquids [252–257], such as water, or silica. These models, that we name 'patchy' models, are based on hard-sphere particles, decorated with a small number M of identical short-ranged square-well attraction sites per particle (sticky spots) at fixed positions [27]. These particles are shown in figure 18 (bottom). Only

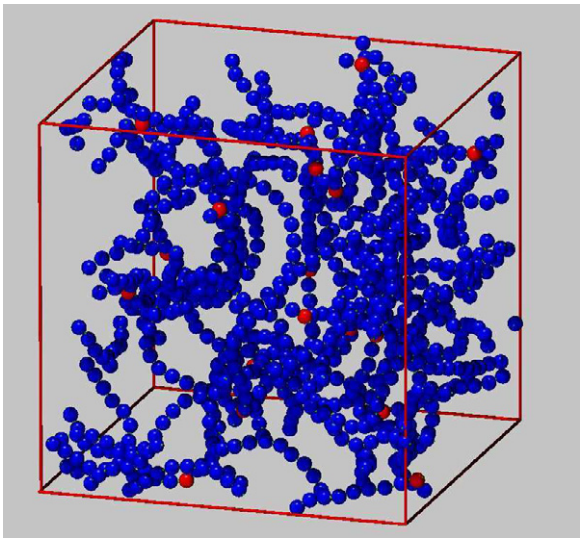

Figure 24. A snapshot from simulations of a gel network made of a mixture of two- and three-coordinated particles of figure 18 with $\langle M \rangle = 2.025$ and $\phi = 0.033$, at very low T. Red particles are those with three neighbours, i.e. the branching points giving rigidity to the gel, while blue particles have two neighbours and provide persistence to the length of network chains. Courtesy of F Sciortino.

when two attractive sites are within the attractive well distance does a bond occur. Multiple bond formation between more than two sites is avoided by a sufficiently small choice of the attractive range δ, namely $\delta < 0.5(\sqrt{5-2\sqrt{3}}-1) \approx 0.119$. Such models are amenable to a thermodynamic perturbation theory treatment, developed by Wertheim [258], as well as numerical simulations [27]. We find that, also in this case, a reduction of the number of sticky spots per particle shifts systematically the critical point and the phase coexistence region towards lower and lower ϕ and T. Moreover, the use of binary mixtures of particles with two and three sticky spots of varying compositions allows us to explore non-integer $\langle M \rangle$. When $\langle M \rangle \to 2$, the critical point also tends continuously to zero, allowing for the possibility to create 'empty' liquids, and accordingly equilibrium gels at very low temperatures. The dynamics of such systems is currently under investigation. However, we report a snapshot from a gel obtained from simulations of such a mixture with low $\langle M \rangle$ in figure 24.

We further note the intriguing result that, while a reduction of the attractive range for spherical potentials has the effect of shifting the critical packing fraction ϕ_c to larger values ($\phi_c \simeq 0.14$ for the van der Waals limit, while $\phi_c \simeq 0.27$ for the Baxter model), the reduction of number of sticky spots goes in the opposite direction, down to $\phi_c = 0$, which is the limit for particles with two sticky spots only. The latter can only form strings and hence no liquid phase. It would be interesting in the near future to complete the phase diagram knowledge with studies of the crystal phases.

It is interesting to point out here, referring the reader to the literature growing at fast pace on the topic, the deep analogy between these models and those 'primitive models' for associating liquids [252–257]. Indeed, recent studies for the dynamics of primitive models for water [259] and silica [260], both models with four bonds per particle, reinforce the robustness of the shape of the N_{max} phase diagram, shown in figure 21 (bottom), suggesting that patchy models for ideal gels and network glass-formers belong to a separate category of liquids with a phase diagram where the glass transition does not end in the coexisting region, as happens for

spherical attractive models, but in a 'new' region of network formation with different dynamical properties. This corresponds to a new topology of phase diagrams, that we schematized in figure 5.

A model for colloidal gels, with directional interactions and more sophisticated than the $N_{\max}$ model, was recently introduced by Del Gado and Kob [261, 262]. In this model, the particle is decorated again by a number of attractive sticky spots (12 sites at fixed geometry). However, a penalty cost in energy is introduced to avoid all attractive spots being simultaneously saturated, through an angular constraint between bonds. Choosing ad hoc the involved parameters (penalty angle, penalty energy), it is possible to equilibrate the system at very low ϕ, as low as 5%, and to study the formation of a gel in equilibrium. The study of the coordination number of the particles reveals that, at low T, most particles forming the network are involved in only two bonds, forming long chains which provide persistence to the network, while a few three-bonded particles provide rigidity to the network, bridging different chains. Hence, this model can be considered, in principle, as an effective mixture of two- and three-coordinated particles with very low $\langle M \rangle$, very similar to that shown in figure 24, so that the absence of phase separation down to very low ϕ is in agreement with the results of Bianchi *et al* [27]. The Del Gado–Kob model is naturally richer in ingredients than the $N_{\max}$ toy model, and allows for a careful study of the length scale dependence of the dynamics. It indeed confirms the main predictions for the characteristic gel properties (i)–(iii). First of all, a very large localization length, that at such low packing fractions can be ten times larger than the particle size, corresponding to the mesh size of the network. Moreover, the static structure factor displays a finite value at $q \to 0$, with a shape similar to that reported in figure 20 for the $N_{\max}$ model, suggesting a significant compressibility of the network and large inhomogeneities in the structure. However, we note here that a large contribution to the $S(q)$ increase at low q comes from the chain contribution [263]. Last but not least, a marked length-scale dependence in the density correlation function is detected [262], again suggesting a distinction between large and small q values, the latter being those significant to characterize in detail the dynamics of the gel network. However, this model has been studied so far at one single packing fraction value, not allowing a clear characterization of the phase diagram and its relation to dynamics. This should be the subject of future studies.

Similar behaviour to patchy colloids and the formation of an equilibrium gel has also been recently reported for dipolar colloids by Blaak *et al* [264], where the dipolar interactions favour the formation of chain-like structures (effectively two-coordinated particles in the language of patchy colloids), and the formation of a network is made possible by the use of slightly elongated dumbbells. The dumbbell geometry allows for branching of the chains at low T, providing structure to the network which indeed is found to display a slow relaxation of the dynamics, in close analogy to studies discussed above where patchy interactions were imposed not via electro-static interactions [28, 261].

Finally, there remains a crucial distinction in all these models between the point where transient networking, i.e. simple percolation, takes place and where gelation, intended as a substantial increase in the relaxation times, occurs. This, as we have seen in detail in the introductory part of this review, is a natural consequence of the decoupling between bond lifetime and network formation at high T. However, once microscopic models for equilibrium gelation are available, it is interesting also to think backwards and find a way to reunify ad hoc percolation and gelation, but maintaining the essential character of physical gelation, that is reversible bond formation. This can be achieved by introducing the specificity of the bond, in order to mimic biological interactions [265, 266], as well to functionalize colloidal particles with DNA strands [267–270]. In the latter case, controlling the length of the chains allows for multiple bond formation at once, so that, despite bonds being reversible, effectively the

bond energy increases. Dynamics of such systems has been recently studied, allowing for detection of gelation in equilibrium very close to the percolation region [271, 272], and with properties close to those of ideal gels (i)–(iii). Interestingly, studies of effective potentials taking into account the specificity of the bonds, manifesting a natural breakdown of pair-wise additivity similar in spirit to the $N_{\max}$ constraint, have been appearing in the literature [273]. This indicates that, for patchy colloids, models have to include some level of complications, either in containing many-body interactions as in the $N_{\max}$ and in the Del Gado–Kob models, or geometrical constraints breaking down the spherical symmetry as in primitive models, or a modification of particle shape as in dipolar dumbbells.

5. Discriminating different gels: static and dynamic features; a closer look at experiments

We have presented here different routes to gelation. As explained in detail, we can clearly distinguish the physical mechanisms at hand resulting in different types of gels. However, in experimental systems, it is not always clear what interactions play a dominant role in determining a particular arrest transition, hence it would be desirable to be able to classify gels according to the different routes proposed here.

For each of the three routes discussed above, we reported a typical image of the gel. In two cases, for the arrested phase separation (figure 11) and the competing interactions (figures 13, 16), experimental examples have been offered. In both cases, simulation snapshots are very similar to the experimental systems, for example in Foffi *et al* [157] for the non-equilibrium gels and in Sciortino *et al* [26] for competing interaction systems (figure 15), where the role of the Bernal spiral as the building block of the gel structure was confirmed. For patchy colloidal gels, experiments are still at the highly non-trivial level of particle production, so that, in this case, only numerical simulations can offer snapshots of the structure, such as in figure 24 (see also [261, 264, 271]). Already by simply looking at these gels, enormous differences can be appreciated by eye. The aim of this paragraph is to provide some further reference framework for classifying gels, based on the observation of static and dynamic features. We have the precise scope to offer specific examples, when available from the literature, to classify the different gels according to our definitions. By no means are we reporting an exhaustive list of experimental works on gels.

We start by discussing structural features of the gels. Structural inhomogeneity, characterized by a non-trivial low-q signal in the scattering intensity, is an ingredient that is often observed in gels, and that allows us to distinguish gels from glasses, the latter being generally structurally homogeneous at all length scales. Tanaka *et al* [206], in a recent attempt to propose a classification scheme for gels, with respect to attractive and repulsive glasses, individuated in the low-angle scattering signal a distinctive gel feature with respect to glasses. However, do the structural inhomogeneities also allow us to distinguish between different types of gels? In chemical gels, the spatial inhomogeneity is instantaneously induced by the formation of random irreversible bonds [274]. However, if reorganization of the bonds is also possible, in colloidal (or thermoreversible) gels, a similar scenario can be found [40, 49]. Indeed, even if particles are left to equilibrate, they may end up forming rather long chains with a few crosslinks giving rigidity to the network. Thus, the system can be locally dense, but with several empty regions, whose typical size is dictated by thermodynamic parameters, such as density, attraction strength etc. Typically, in these conditions, a significant signal at low q in the static structure factor is observed.

However, it is important to be able to distinguish an equilibrium finite value of the compressibility, i.e. a finite value of $S(q \rightarrow 0)$, from an incipient phase separation, where

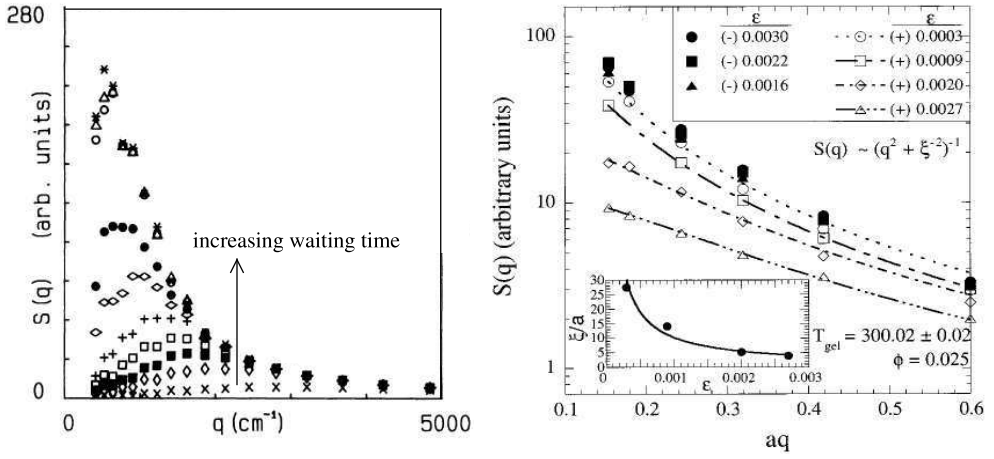

Figure 25. Reprinted with permission from [70] and [49]. Copyright 1992 and 2001 by the American Physical Society. Two different experimental reports on the low-q behaviour of the $S(q)$ for (left panel) a DLCA gel as a function of waiting time, varying from 722 to 60 753 s from bottom to top. The last three curves ($t > 18\,000$ s) show a saturation effect. Right panel, a thermoreversible gel of adhesive spheres approaching the gel transition with $\epsilon = (T - T_{\rm gel})/T_{\rm gel}$. Here $a = 40$ nm is the particle radius. Curves are fits to the scaling $S(q) \sim (q^2 + \xi^{-2})^{-1}$ in the fluid phase (open symbols), with ξ a (phenomenological) correlation length. In the gel phase (full symbols), $S(q)$ does not change further.

eventually $S(q = 0) \to \infty$, or from an interrupted one, where the initial coarsening (i.e. a growing peak at finite small q in $S(q)$) is stopped at some point. To carefully assess this issue, in principle, the time behaviour of the low-q region of $S(q)$ should be monitored during aggregation, as done in the remarkable experiment by Carpineti and Giglio [70] for the case of colloidal DLCA. The behaviour of $S(q)$ was shown to obey growth rules similar to spinodal decomposition of fractal aggregates. The growth of $S(q)$ stops at large waiting times, as shown in figure 25 (left panel). This behaviour was interpreted as an imprinting of phase separation on irreversible DLCA [275]. Cipelletti *et al* also reported the time evolution of the low-q behaviour of $S(q)$ for polystyrene DLCA-like gels [276], where aggregation proceeds with time until gelation is reached. At the gel point, $S(q)$ varies only on a timescale of days, apparently towards a more locally compact structure [276].

To include the reversibility of the bonds in the picture, we report in figure 25 (right panel) the temperature dependence of $S(q)$ for thermoreversible adhesive spheres, studied by Varadan and Solomon [49], in the vicinity of the gel temperature. In this system, a marked increase of the low-q signal is observed, becoming more and more pronounced with the proximity of the transition, and can be well fitted by an Ornstein–Zernike form (lines in the figure), signalling the approach to criticality with an increasing correlation length. However, when the gel point is reached, the structure freezes, so that phase separation is interrupted by gelation. More experimental studies of colloidal gels at finite attraction strengths (where bonds are reversible) should be carried out to properly monitor, in time, the arrested phase separation scenario. In this way, an often invoked unifying picture between DLCA and colloidal gels could be ultimately proven. A detailed $S(q)$ versus time experiment would also be desirable for uncharged PMMA spheres (or similar well characterized systems), especially to differentiate the two scenarios above and below $T_{\rm g}^{\rm sp}$, where the glass line meets the spinodal line (see figure 3): in the former case phase separation should proceed without arrest, with a monotonic increase of $S(q \to 0)$

over time, while in the latter phase separation is interrupted by gelation, similarly to what is observed in the experiments mentioned above. In this way, also the question of how the glass line is affected by crossing the spinodal region could be tackled.

The examples of low-q behaviour of $S(q)$ reported above refer to a non-equilibrium approach to gelation, both for irreversible and reversible bond formation. On the other hand, if gelation is approached in equilibrium, through one of the routes anticipated in section 2, no hint of spinodal decomposition scaling in $S(q)$ should be present. Still, however, some remarkable low-q features of $S(q)$ are expected approaching the gel phase. When competing interactions are at hand, for example a long-range repulsion in addition to a short-range attraction, a stable pre-peak emerges at a finite wavevector q_c^* much lower than that typical of a nearest-neighbour peak. This was discussed in section 4.2 and a typical $S(q)$ was shown in the case of lysozyme (figure 14). Similar behaviour was also reported for charged PMMA spheres by Segrè *et al* [167]. Concerning simulations and theory, this is a well established phenomenon as we discussed previously. What remains to be established is a theoretical approach able to describe in detail the evolution of the cluster peak positions with changing screening length and energy strength, as well as how a variation of the potential parameters tunes a crossover from micro- to macrophase separation [277]. This aspect could be particularly interesting for those systems where the screening length changes rapidly with particle concentration so that different scenarios may be observed at different densities, such as in lysozyme [174]. Finally, in the case of gels formed by patchy particles, no experimental results are yet available. However simulations of different models [245, 262] agree in showing a finite increase in $S(q)$ at $q \to 0$, signalling a finite compressibility increase associated with the formation of an open network. This is thus different from the presence of a peak at finite q as well as from a critical-like scenario.

Studies of the dynamical density fluctuations on approaching the gel line are crucial to characterize the arrest transition. A pioneering work putting forward the analogy between gel and glass transition was carried out by Ren and Sorensen [278], who studied a thermoreversible gel-forming system (gelatin) by dynamic light scattering, identifying two relaxations that would be the analogues of the α and β relaxation in glasses [20]. The α relaxation equivalence was identified with a stretched exponential decay approaching the gel point, while the β relaxation was associated with the so-called 'gel mode', i.e. a power-law decay at the gel transition which is typical of chemical gels [37, 279]. Such a power-law decay was also found in irreversible colloidal gels [280]. Most importantly, Ren and Sorensen discussed the importance of wavelength dependence in relaxation of gels with respect to glasses, and highlighted the importance of the low q region to detect non-ergodicity in gels. They anticipated the idea that, while glasses are localized around nearest-neighbour lengths, in gels this length should be much larger than a particle diameter, calling for experiments at different wavelengths to study the different dynamics of gels and glasses. As discussed in sections 3 and 4, this concept is crucial in discussing gelation and calls for the need to use also small-angle and ultra-small-angle scattering ranges to properly address colloidal gelation.

For fractal colloidal gels close to the DLCA limit (i.e. at very low ϕ and $d_f \approx 1.9$), dynamics of density fluctuations was studied by Krall and Weitz [281] and a significant q-dependence was reported in the non-ergodic behaviour. In figure 26, density auto-correlation functions $F_q(t)$ are shown for different packing fractions (from 5×10^{-3} to 1.7×10^{-4}) and scattering vector values (from $0.08q\sigma$ to $0.42q\sigma$) lying in the low-q peak region, well below the static structure factor peak. In this way, only the cluster–cluster correlations are probed. Data show a remarkable q-dependence with packing fraction. At the smallest ϕ the system remains ergodic, while with increasing ϕ a non-ergodic behaviour is observed, which is much more evident for smaller than for larger q. The observation time is indeed 100 s, and hence

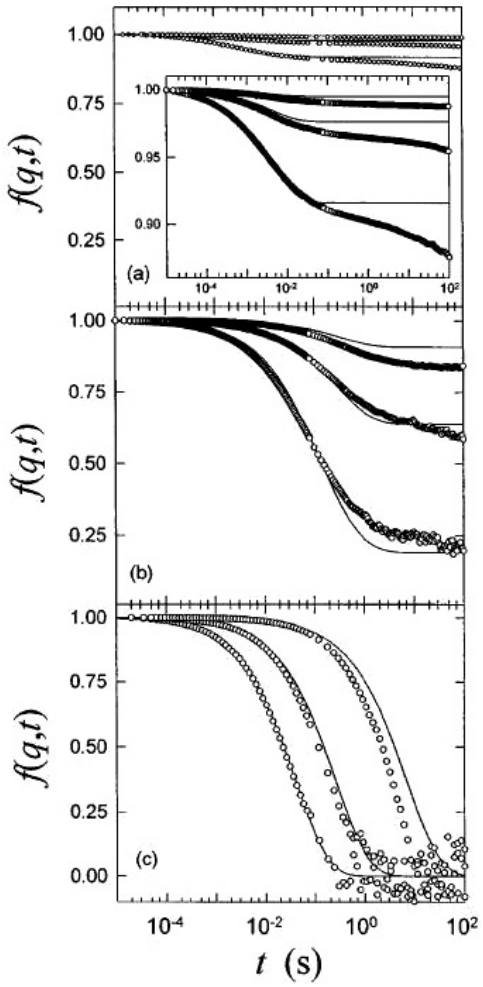

Figure 26. Reprinted with permission from [281]. Copyright 1998 by the American Physical Society. Density correlation functions $F_q(t)$ (labelled as $f(q, t)$ in the original paper and therefore in the y-axis) for a fractal gel at $\phi = 5 \times 10^{-3}$ (a), 1.5×10^{-3} (b) and 1.7×10^{-4} (c) for various wavevectors ranging from $\sim 0.08 q\sigma$ to $\sim 0.42 q\sigma$.

the larger ϕ-value state points (a), (b) can be considered as gels. The relaxation law of the scattering curves is well described by a stretched exponential with exponent ≈ 0.66, which appears to be valid for all studied q and ϕ values. Interestingly, given the strong q-variation of relaxation plateau and relaxation time, it should be possible, in principle, at certain length-scales to observe a (quasi-) ergodic behaviour at large q and a non-ergodic one at small q. The fact that the gel transition is strongly wavevector dependent is discussed by Krall and Weitz in the conclusions [281] and coincides with what is found in simulations of colloidal gels, in the case of competing interactions (figure 17) as well as for patchy colloids (figure 21). Moreover, it agrees with the q-dependent scenario put forward in simulations of chemical gels [91] (figures 7 and 8).

Thus, an interesting aspect of the gel dynamics is the wavelength dependence of the relaxation. However, it is much more common to find in the literature scattering data at fixed angle, reporting a change in behaviour as a function of the proximity to the transition,

e.g. varying attraction strength or density. This is a valid approach for example in glasses, where localization acts at all relevant length-scales, but it can provide only partial information about gelation. In general, various relaxation decays are observed: from stretched or log-like to compressed or single exponentials. It still appears difficult to properly associate these features with inter-particle potentials and length-scale of observation. The DLCA-like gel studied by Krall and Weitz was well described by stretched exponentials at low q, while it was found to turn to a compressed exponential with compressing exponent $\approx$1.5 at large q in the aging regime by Cipelletti and co-workers [276]. On the other hand, the thermoreversible adhesive spheres of Varadan and Solomon [49] are also reported to approach gelation at low q in a stretched exponential manner, while in the gel regime a two-step decay is observed where the departure from the plateau is exponential. The same authors offer an interpretation, aimed to explain the different results for the two cases, which is based on the interactions involved. They suggest that the different strengths of attraction involved in the gel formation process (irreversible in one case, giving rise to a network with small d_f, reversible in the other with more compact structure) might be the key for explaining the different features. Interestingly, in both cases, even in the gel phase, ergodicity is restored at very long times, probably due to the chosen scattering vector, that is too large to detect the length scale of the network. It would be highly desirable to be able to associate with specific interactions a certain behaviour of $F_q(t)$ and in this respect simulation studies may be valuable [91, 262]. We note that the shape of the correlation functions calculated from simulations may be affected by the choice of the microscopic dynamics (e.g. Newtonian versus Brownian) and by neglecting hydrodynamics interactions. A more detailed analysis of $F_q(t)$ both on approaching the gel transition and in its wavevector dependence should be carried out for ideal gel models: a DLCA gel, an arrested phase separation one, an equilibrium one from competing interactions and one from patchy particles. A comparison of these studies could help to characterize the relaxation in terms of the different gelation mechanisms.

Finally, we briefly report on visco-elastic gel properties. This is the subject for which plenty of experiments are available, as a visco-elasticity study is the most natural way to characterize a gel, while numerical simulations are rare due to the very demanding computational effort. For chemical gels [274], the viscosity coefficient on approaching the gelation/percolation transition, as well the elastic modulus within the gel phase, are found to obey a power law behaviour, whose exponents can sensitively vary among different samples. For the viscosity, $\eta \sim (p_c - p)^k$, with k varying in the range 0.6–1.5, while for the elastic modulus $G \sim (p - p_c)^t$, with $1.9 \leqslant t \leqslant 3$. Several models have been used to rationalize these differences, pointing to possible different universality classes due to different bonding units or bond rigidity. For colloidal gels, a power law behaviour as a function of increasing packing fraction is found. In the case of the fractal gel studied by Krall and Weitz [281], the elastic modulus exponent was determined to be $t \sim 3.9$. For thermoreversible gels, Grant and Russel [46] found an exponent close to three, while Rueb and Zukoski [48, 282] found a slightly different functional form, but still compatible with a power-law increase with packing fraction with different exponents, for a similar thermoreversible suspension. For PMMA particles with added polymers, it was found that the power-law exponent varies with the range of depletion attraction, increasing from $\sim$2.1 to $\sim$3.3 as the attraction range is decreased [283]. The onset of elasticity in such colloidal gels has been interpreted in terms of rigidity percolation [284, 283] and the change of exponents attributed to an increase of the gel resistance to bond-stretching for large ranges, well described by the exponent $t \approx 2.1$, to bond-bending for shorter ranges, where $t \approx 3.3$. Hence the difference in the exponents should be associated with different stress-bearing properties in the gel network [12]. We also mention a study of a DLCA-like gel, at moderate densities $\phi \simeq 0.2$, where a power-law increase of the moduli was observed as a

function of time during aggregation [280]. From viscosity measurements, a similar scenario can be inferred from micellar solutions [52, 141], since viscosity is found at first to undergo a sudden increase close to the percolation packing fraction, later followed by a true divergence close to the glassy behaviour at large ϕ. Also, this suggests that in attractive systems at first there is the establishment of a network with elastic properties, only later, at much higher density, crossing over to a standard glass behaviour.

6. Conclusions and perspectives

In this review we have proposed a classification of colloidal gels. We have highlighted the difference between transient percolation and gelation for physical gels and we have discussed three different routes to gelation. We have also tried to address how it should be possible to discriminate among them.

As for colloidal glasses, also in the case of colloidal gelation, the interplay between simulation, theory and experiments is starting to provide a coherent picture of arrest at low packing fraction. In the case of spherically symmetric potentials in which excluded volume repulsion is complemented only by attraction, there is now growing consensus that arrested phase separation is the mechanism driving gelation. For competing interactions, combined and closely related experimental, theoretical and numerical studies are also providing a coherent view of the arrest processes involved. Finally, for patchy colloids it is foreseeable that the same will happen in the near future, when functionalized or patchy particles will become readily available for experimental studies.

A final comment is owed to the relationship between gels and glasses. Gels and glasses have often been viewed in an unifying framework due to unambiguous similarities in the arrest transition, i.e. the presence of long-time plateaus in the relaxation observables which can be also well fitted by power laws [60, 167]. For this reason, MCT-like approaches have also been often applied to describe the gel transition [114, 158]. However, we pointed out in this review the limits of such applications, both in relation to the arrested-phase separation scenario and for the development of a cluster MCT. While both gels and attractive glasses undergo arrest dictated by bond formation, many differences are present. In our opinion, the main difference is that arrest occurs within the presence of a spanning network in the gel case (thus with a large localization length dictated by the mesh size of the gel) and through local cages arising from the short-range bonds in the attractive glass case (where the localization length is provided by the bond distance). Consequently, a completely different scenario arises in the non-ergodic behaviour of gels, shifting the interesting q-range of arrest to values that are smaller than that of glasses (more than two orders of magnitude in the case of attractive glasses). A notable case is, in this context, the Wigner glass, which can be made either of particles or of clusters. In this review, we have proposed to classify it as a glass, despite the low density, due to the absence of connectivity and of attractive interactions in stabilizing the arrested disordered structure. However, we might speculate that the Wigner glass is an intermediate state between gels and glasses as it should share some properties with gels (structural inhomogeneity, large localization length) and some with glasses (low shear modulus, repulsive caging). Therefore, a detailed study of the Wigner dynamical arrest transition, also focusing on the q-dependence of the density correlation functions, will be important to clearly establish its classification.

Throughout this review, we have pointed out several times that gelation is strongly associated with a connectivity transition. Hence, if the lifetime of the bonds is sufficiently long, ergodicity should strictly be broken starting from $q = 0$. Within the gel region, larger and larger q will display then non-ergodic behaviour, but for each q at a different distance from the $q = 0$-gel transition. It will be important to characterize this aspect, firstly for chemical

gels [285], and then possibly for physical gels of various kinds. A closer look should be taken at the low-q behaviour of $S(q)$ as well as of $F_q(t)$, to definitely identify the distinctive features of gels, and the peculiar characteristics arising from the different arrest mechanisms. To develop an ideal theory of gelation, previous studies on reversible polymer gelation should be taken into account [57], combined with the central idea of the $q = 0$-transition at long-lived percolation. Clearly, the lack of a predictive framework constitutes a problem in the present-day study of colloidal gelation.

On the other hand, the close similarity between gels and glasses, both being phenomena of dynamical arrest, suggests to look for the characteristic arrest signatures also in gels. In particular, in close analogy with investigations in colloidal glasses [286], recent, intense activity is aiming to characterize dynamical heterogeneities of colloidal gels. Through diffusing wave spectroscopy and time resolved correlation techniques [287, 9], confocal microscopy experiments [178, 179], and simulations [288, 289, 87], the complexity of gels emerges also in terms of different populations of slow and fast particles, which become more and more evident approaching the gel transition, and remarks a close analogy of both gel and glass transition in terms of dynamic cooperativity. Such studies are extremely useful for the establishment of a unifying theoretical framework of a (generic) dynamical arrest transition, although, again, differences are expected among the different mechanisms. For example, we expect that, for an arrested phase-separated gel, dynamical heterogeneities should look very different from those arising in equilibrium gels.

This review shows that the study of colloidal gels is still challenging, despite the progress that has been made in the last decade. Colloidal gelation is a rich field of scientific investigation, which offers the possibility to develop new theories and models, as well to design new classes of materials (as in the case of patchy particles). The progress in the study of colloidal gelation will hopefully also provide a deeper understanding of several protein-related aggregation processes [244, 15, 290].

Acknowledgments

First of all it is a pleasure to thank Francesco Sciortino and Piero Tartaglia for many discussions on colloids, glasses and gels, as well as for illuminating comments on this manuscript. Also, I deeply thank Hartmut Löwen for suggesting that I write a review on this topic, and Silvia Corezzi and Gi-Ra Yi for providing me with figures. Warmest thanks to all colleagues who granted me permission to reproduce their figures as well as to the close collaborators who helped me, with their work, to understand relevant aspects of colloidal gelation: I Saika Voivod, G Foffi, S Mossa, E Bianchi, J Largo, A J Moreno, E La Nave, C De Michele, S Buldyrev, F Ciulla and B Ruzicka. I am also grateful to C N Likos, P J Lu and F Cardinaux for many stimulating discussions. I acknowledge support from MIUR-Prin and Marie Curie Network on Dynamical Arrest of Soft Matter and Colloids MRTN-CT-2003-504712.

References

[1] See FP6 Marie Curie network on dynamical arrest http://www.arrestedmatter.net
[2] Prasad V, Semwogerere D and Weeks E R 2007 *J. Phys.: Condens. Matter* **19** 3102
[3] Manoharan V N, Elsesser M T and Pine D J 2003 *Science* **301** 483–7
[4] Yethiraj A and van Blaaderen A 2003 *Nature* **421** 513–7
[5] van Blaaderen A 2006 *Nature* **439** 545
[6] Likos C N 2001 *Phys. Rep.* **348** 267–439
[7] Derjaguin B V and Landau L V 1941 *Acta Physicochim. USSR* **14** 633
Verwey J W and Overbeek J T 1948 *Theory of Stability of Lyophobic Colloids* (Amsterdam: Elsevier)

[8] Asakura S and Oosawa F 1958 *J. Polym. Sci.* **33** 183–92
[9] Cipelletti L and Ramos L 2005 *J. Phys.: Condens. Matter* **17** 253
[10] Dawson K A 2002 *Curr. Opin. Colloid Interface Sci.* **7** 218
[11] Sciortino F and Tartaglia P 2005 *Adv. Phys.* **54** 471–524
[12] Trappe V and Sandkühler P 2004 *Curr. Opin. Colloid Interface Sci.* **8** 494–500
[13] Poon W C K 1998 *Curr. Opin. Colloid Interface Sci.* **3** 593
[14] Piazza R 2000 *Curr. Opin. Colloid Interface Sci.* **5** 38–43
[15] Sear R P 2006 *Curr. Opin. Colloid Interface Sci.* **11** 35
[16] Groenewold J and Kegel W K 2003 *J. Phys. Chem.* B **105** 11702–9
[17] Dinsmore A D and Weitz D A 2002 *J. Phys.: Condens. Matter* **14** 7581–97
[18] Campbell A I, Anderson V J, van Duijneveldt J and Bartlett P 2005 *Phys. Rev. Lett.* **94** 208301
[19] Flory P J 1971 *Principles of Polymer Chemistry* (Ithaca, NY: Cornell University Press)
[20] Götze W 1991 *Liquids, Freezing and the Glass Transition* (Amsterdam: North-Holland) pp 287–503
[21] Sciortino F, Mossa S, Zaccarelli E and Tartaglia P 2004 *Phys. Rev. Lett.* **93** 055701
[22] Manley S, Wyss H, Miyazaki K, Conrad J, Trappe V, Kaufman L J, Reichman D R and Weitz D A 2005 *Phys. Rev. Lett.* **94** 238302
[23] Zaccarelli E, Sciortino F, Buldyrev S V and Tartaglia P 2004 *Short-Ranged Attractive Colloids: What is the Gel State?* (Amsterdam: Elsevier) pp 181–94
[24] Foffi G, De Michele C, Sciortino F and Tartaglia P 2005 *Phys. Rev. Lett.* **94** 078301
[25] Vicsek T 1989 *Fractal Growth Phenomena* (Singapore: World Scientific)
[26] Sciortino F, Tartaglia P and Zaccarelli E 2005 *J. Phys. Chem.* B **109** 21942
[27] Bianchi E, Largo J, Tartaglia P, Zaccarelli E and Sciortino F 2006 *Phys. Rev. Lett.* **97** 168301
[28] Zaccarelli E, Buldyrev S V, La Nave E, Moreno A J, Saika-Voivod I, Sciortino F and Tartaglia P 2005 *Phys. Rev. Lett.* **94** 218301
[29] *Encyclopædia Britannica* 2007 http://www.britannica.com/eb/article-9036313/gel
[30] Corezzi S, Palmieri L, Kenny J M and Fioretto D 2005 *J. Phys.: Condens. Matter* **17** 3557
[31] Flory P J 1941 *J. Am. Chem. Soc.* **63** 3083
[32] Stockmayer W H 1943 *J. Chem. Phys.* **11** 45
[33] Stockmayer W H 1944 *J. Chem. Phys.* **12** 125
[34] Stauffer D and Aharony A 1992 *Introduction to Percolation Theory* 2nd edn (London: Taylor and Francis)
[35] Corezzi S, Fioretto D, Puglia D and Kenny J M 2003 *Macromolecules* **36** 5271
[36] Corezzi S, Comez L, Monaco G, Verbeni R and Fioretto D 2006 *Phys. Rev. Lett.* **96** 255702
[37] Martin J E and Wilcoxon J P 1988 *Phys. Rev. Lett.* **61** 373–6
[38] Martin J E, Adolf D and Wilcoxon J P 1988 *Phys. Rev. Lett.* **61** 2620–3
[39] Martin J E, Wilcoxon J and Odinek J 1991 *Phys. Rev.* A **43** 858–72
[40] Ikkai F and Shibayama M 1999 *Phys. Rev. Lett.* **82** 4946–9
[41] del Gado E, Fierro A, de Arcangelis L and Coniglio A 2003 *Europhys. Lett.* **63** 1–7
[42] Ilett S M, Orrock A, Poon W C K and Pusey P N 1995 *Phys. Rev.* E **51** 1344–52
[43] Poon W C K, Pirie A D, Haw M D and Pusey P N 1997 *Physica* A **235** 110–9
[44] Verhaegh N A M, Asnaghi D, Lekkerkerker H N W, Giglio M and Cipelletti L 1997 *Physica* A **242** 104–18
[45] Segrè P N, Prasad V, Schofield A B and Weitz D A 2001 *Phys. Rev. Lett.* **86** 6042–5
[46] Grant M C and Russel W B 1993 *Phys. Rev.* E **47** 2606–14
[47] Verduin H and Dhont J K G 1995 *J. Colloid Interface Sci.* **172** 425–37
[48] Rueb C J and Zukoski C F 1997 *J. Rheol.* **41** 197
[49] Solomon M J and Varadan P 2001 *Phys. Rev.* E **63** 051402
[50] Sztucki M, Narayanan T, Belina G, Moussaïd A, Pignon F and Hoekstra H 2006 *Phys. Rev.* E **74** 051504
[51] Vlassopoulos D, Pakula T, Fytas G, Pitsikalis M and Hadjichristidis N 1999 *J. Chem. Phys.* **111** 1760
[52] Lafleche F, Durand D and Nicolai T 2002 *Macromolecules* **36** 1331
[53] Lo Verso F, Likos C N, Mayer C and Löwen H 2006 *Phys. Rev. Lett.* **96** 187802
[54] Michel E, Filali M, Aznar R, Porte G and Appell J 2000 *Langmuir* **16** 8702–11
[55] Manno M, San Biagio P L and Palma M U 2004 *Proteins Struct. Funct. Bioinformatics* **55** 169–76
[56] Pan W C, Kolomeisky A B and Vekilov P G 2005 *J. Chem. Phys.* **122** 174905
[57] Rubinstein M and Dobrynin A V 1999 *Curr. Opin. Colloid Interface Sci.* **4** 83
[58] Torquato S 2002 *Random Heterogeneous Materials: Microstructure and Macroscopic Properties* (New York: Springer)
[59] Rubistein M and Semenov A N 1998 *Macromolecules* **31** 1386–97
[60] Kumar S K and Douglas J F 2001 *Phys. Rev. Lett.* **87** 188301
[61] Coniglio A and Klein W 1980 *J. Phys. A: Math. Gen.* **13** 2775

[62] Coniglio A, Stanley H and Klein W 1979 *Phys. Rev. Lett.* **42** 518
[63] Hill T L 1987 *An Introduction to Statistical Thermodynamics* (New York: Dover)
[64] Wales D J and Doye J P K 1997 *J. Phys. Chem.* A **101** 5111
[65] Mossa S, Sciortino F, Tartaglia P and Zaccarelli E 2004 *Langmuir* **20** 10756–63
[66] Sciortino F, Buldyrev S, De Michele C, Ghofraniha N, La Nave E, Moreno A, Mossa S, Tartaglia P and Zaccarelli E 2005 *Comput. Phys. Commun.* **169** 166–71
[67] Cardinaux F, Gibaud T, Stradner A and Schurtenberger P 2007 submitted
[68] Cates M E, Fuchs M, Kroy K, Poon W C K and Puertas A M 2004 *J. Phys.: Condens. Matter* **16** 4861
[69] Weitz D A and Oliveria M 1984 *Phys. Rev. Lett.* **52** 1433–6
[70] Carpineti M and Giglio M 1992 *Phys. Rev. Lett.* **68** 3327–30
[71] Krall A H and Weitz D A 1998 *Phys. Rev. Lett.* **80** 778–81
[72] Cipelletti L, Manley S, Ball R C and Weitz D A 2000 *Phys. Rev. Lett.* **84** 2275–8
[73] Ramos L and Cipelletti L 2005 *Phys. Rev. Lett.* **94** 158301
[74] Manley S, Cipelletti L, Trappe V, Bailey A E, Christianson R J, Gasser U, Prasad V, Segre P N, Doherty M P, Sankaran S, Jankovsky A L, Shiley B, Bowen J, Eggers J, Kurta C, Lorik T and Weitz D A 2004 *Phys. Rev. Lett.* **93** 108302
[75] Manley S, Skotheim J M, Mahadevan L and Weitz D A 2005 *Phys. Rev. Lett.* **94** 218302
[76] Manley S, Davidovitch B, Davies N R, Cipelletti L, Bailey A E, Christianson R J, Gasser U, Prasad V, Segre P N, Doherty M P, Sankaran S, Jankovsky A L, Shiley B, Bowen J, Eggers J, Kurta C, Lorik T and Weitz D A 2005 *Phys. Rev. Lett.* **95** 048302
[77] Condre J M, Ligoure C and Cipelletti L 2007 *J. Stat. Mech.* **2** 02010
[78] Kolb M, Botet R and Jullien R 1983 *Phys. Rev. Lett.* **51** 1123–6
[79] Meakin P 1983 *Phys. Rev. Lett.* **51** 1119–22
[80] Vicsek T and Family F 1984 *Phys. Rev. Lett.* **52** 1669–72
[81] Gimel J C, Nicolai T and Durand D 1999 *J. Sol–Gel Sci. Technol.* **15** 129–36
[82] Gimel J C, Durand D and Nicolai T 1995 *Phys. Rev.* B **51** 11348–57
[83] Hasmy A, Foret M, Pelous J and Jullien R 1993 *Phys. Rev.* B **48** 9345–53
[84] Rottereau M, Gimel J C, Nicolai T and Durand D 2004 *Eur. Phys. J.* E **15** 133–40
[85] Rottereau M, Gimel J C, Nicolai T and Durand D 2004 *Eur. Phys. J.* E **15** 141–8
[86] Charbonneau P and Reichman D R 2007 *Phys. Rev.* E **75** 050401
[87] Hurtado P I, Berthier L and Kob W 2007 *Phys. Rev. Lett.* **98** 135503
[88] Puertas A M, Fuchs M and Cates M E 2002 *Phys. Rev. Lett.* **88** 098301
[89] Puertas A M, Fuchs M and Cates M E 2003 *Phys. Rev.* E **67** 031406
[90] Zaccarelli E, Foffi G, Sciortino F and Tartaglia P 2003 *Phys. Rev. Lett.* **91** 108301
[91] Saika-Voivod I, Zaccarelli E, Sciortino F, Buldyrev S V and Tartaglia P 2004 *Phys. Rev.* E **70** 041401
[92] Zaccarelli E, Sciortino F and Tartaglia P 2004 *J. Phys.: Condens. Matter* **16** 4849–60
[93] Stradner A, Sedgwick H, Cardinaux F, Poon W C K, Egelhaaf S U and Schurtenberger P 2004 *Nature* **432** 492–5
[94] Puertas A M, Fuchs M and Cates M E 2004 *J. Phys. Chem.* B **109** 6666
[95] Henrich O, Puertas A M, Sperl M, Baschnagel J and Fuchs M 2007 *Preprint* condmat/0705.0637
[96] Puertas A M, Fuchs M and Cates M E 2007 *J. Phys.: Condens. Matter* **19** 205140
[97] Lai S K, Ma W J, van Megen W and Snook I K 1997 *Phys. Rev.* E **56** 766–9
[98] Bosse J and Wilke S D 1998 *Phys. Rev. Lett.* **80** 1260–3
[99] Bonn D, Tanaka H, Wegdam G, Kellay H and Meunier J 1999 *Europhys. Lett.* **45** 52–7
[100] Ruzicka B, Zulian L and Ruocco G 2004 *Phys. Rev. Lett.* **93** 258301
[101] Kapnistos M, Vlassopoulos D, Fytas G, Mortensen K, Fleischer G and Roovers J 2000 *Phys. Rev. Lett.* **85** 4072–5
[102] Stiakakis E, Vlassopoulos D, Likos C N, Roovers J and Meier G 2002 *Phys. Rev. Lett.* **89** 208302
[103] Nicolai T, Lafleche F and Gibaud A 2004 *Macromolecules* **37** 8066–71
[104] Laurati M, Stellbrink J, Lund R, Willner L, Richter D and Zaccarelli E 2005 *Phys. Rev. Lett.* **94** 195504
[105] Zaccarelli E, Mayer C, Asteriadi A, Likos C N, Sciortino F, Roovers J, Iatrou H, Hadjichristidis N, Tartaglia P, Löwen H and Vlassopoulos D 2005 *Phys. Rev. Lett.* **95** 268301
[106] Foffi G, Sciortino F, Tartaglia P, Zaccarelli E, Verso F L, Reatto L, Dawson K A and Likos C N 2003 *Phys. Rev. Lett.* **90** 238301
[107] Zaccarelli E *et al* Unpublished results
[108] Pusey P N and van Megen W 1987 *Phys. Rev. Lett.* **59** 2083–6
[109] van Megen W and Underwood S M 1993 *Phys. Rev. Lett.* **70** 2766–9
[110] Williams S R, Snook I K and van Megen W 2001 *Phys. Rev.* E **64** 021506

[111] Zaccarelli E, Foffi G, Sciortino F, Tartaglia P and Dawson K A 2001 *Europhys. Lett.* **55** 157–63
[112] Vrij A 1976 *Pure Appl. Chem.* **48** 471
[113] Fabbian L, Götze W, Sciortino F, Tartaglia P and Thiery F 1999 *Phys. Rev.* E **59** 1347–50
[114] Bergenholtz J and Fuchs M 1999 *Phys. Rev.* E **59** 5706–15
[115] Dawson K A, Foffi G, Fuchs M, Götze W, Sciortino F, Sperl M, Tartaglia P, Voigtmann T and Zaccarelli E 2001 *Phys. Rev.* E **63** 011401
[116] Sciortino F 2002 *Nat. Mater.* **1** 145–68
[117] Frenkel D 2002 *Science* **296** 65–6
[118] Pham K N, Puertas A M, Bergenholtz J, Egelhaaf S U, Moussaïd A, Pusey P N, Schofield A B, Cates M E, Fuchs M and Poon W C K 2002 *Science* **296** 104–6
[119] Eckert T and Bartsch E 2002 *Phys. Rev. Lett.* **89** 125701
[120] Mallamace F, Gambadauro P, Micali N, Tartaglia P, Liao C and Chen S H 2000 *Phys. Rev. Lett.* **84** 5431–4
[121] Chen W, Mallamace F, Glinka C J, Fratini E and Chen S 2003 *Phys. Rev.* E **68** 041402
[122] Pham K N, Egelhaaf S U, Pusey P N and Poon W C K 2004 *Phys. Rev.* E **69** 1–13
[123] Pontoni D, Narayanan T, Petit J M, Grübel G and Beysens D 2003 *Phys. Rev. Lett.* **90** 188301
[124] Grandjean J and Mourchid A 2004 *Europhys. Lett.* **65** 712–8
[125] Pham K N, Petekidis G, Vlassopoulos D, Egelhaaf S U, Pusey P N and Poon W C K 2006 *Europhys. Lett.* **75** 624–30
[126] Foffi G, Dawson K A, Buldrey S V, Sciortino F, Zaccarelli E and Tartaglia P 2002 *Phys. Rev.* E **65** 050802
[127] Zaccarelli E, Foffi G, Dawson K A, Buldrey S V, Sciortino F and Tartaglia P 2002 *Phys. Rev.* E **66** 041402
[128] Zaccarelli E, Foffi G, Dawson K A, Sciortino F and Tartaglia P 2001 *Phys. Rev.* E **63** 031501
[129] Puertas A M, Zaccarelli E and Sciortino F 2005 *J. Phys.: Condens. Matter* **17** L271–7
[130] Narayanan T, Sztucki M, Belina G and Pignon F 2006 *Phys. Rev. Lett.* **96** 258301
[131] Götze W and Sperl M 2002 *Phys. Rev.* E **66** 011405
[132] Sperl M 2003 *Phys. Rev.* E **68** 031405
[133] Sciortino F, Tartaglia P and Zaccarelli E 2003 *Phys. Rev. Lett.* **91** 268301
[134] Bartsch E, Antonietti M, Schupp W and Sillescu H 1992 *J. Chem. Phys.* **97** 3950–63
[135] Liu Y and Pandey R B 1996 *J. Chem. Phys.* **105** 825–36
[136] Jin J M, Parbhakar K, Dao L H and Lee K H 1996 *Phys. Rev.* E **54** 997–1000
[137] Liu Y and Pandey R B 1997 *Phys. Rev.* B **55** 8257–66
[138] Gimel J C, Nicolai T and Durand D 2001 *Eur. Phys. J.* E **5** 415–22
[139] Gimel J C, Nicolai T and Durand D 2002 *Phys. Rev.* E **66** 061405
[140] Del Gado E, Fierro A, de Arcangelis L and Coniglio A 2004 *Phys. Rev.* E **69** 051103
[141] Mallamace F, Chen S H, Coniglio A, de Arcangelis L, Del Gado E and Fierro A 2006 *Phys. Rev.* E **73** 020402(R)
[142] Bergenholtz J, Poon W C K and Fuchs M 2003 *Langmuir* **19** 4493–503
[143] Lekkerkerker H N W, Poon W C K, Pusey P N, Stroobants A and Warren P B 1992 *Europhys. Lett.* **20** 559–64 414
[144] Asherie N, Lomakin A and Benedek G B 1996 *Phys. Rev. Lett.* **77** 4832–5
[145] Anderson V J and Lekkerkerker H N W 2002 *Nature* **416** 811–5
[146] Noro M G and Frenkel D 2000 *J. Chem. Phys.* **113** 2941–4
[147] Vliegenthart G A and Lekkerkerker H N W 2000 *J. Chem. Phys.* **12** 5364–9
[148] Foffi G and Sciortino F 2006 *Phys. Rev.* E **74** 050401
[149] Hansen J P and MacDonald I R 2006 *Theory of Simple Liquids* 3rd edn (London: Academic)
[150] Miller M A and Frenkel D 2003 *Phys. Rev. Lett.* **90** 135702
[151] Miller M A and Frenkel D 2004 *J. Chem. Phys.* **121** 535–45
[152] Foffi G, Sciortino F, Zaccarelli E and Tartaglia P 2004 *J. Phys.: Condens. Matter* **16** 3791
[153] Poulin P, Bibette J and Weitz D A 1999 *Eur. Phys. J.* B **7** 277–81
[154] Sciortino F, Bansil R, Stanley H E and Alstrøm P 1993 *Phys. Rev.* E **47** 4615–8
[155] Sappelt D and Jäckle J 1997 *Europhys. Lett.* **37** 13–8
[156] Onuki A and Puri S 1999 *Phys. Rev.* E **59** 1331–4
[157] Foffi G, De Michele C, Sciortino F and Tartaglia P 2005 *J. Chem. Phys.* **122** 4903
[158] Kroy K, Cates M E and Poon W C 2004 *Phys. Rev. Lett.* **92** 148302
[159] Sedgwick H, Kroy K, Salonen A, Robertson M B, Egelhaaf S U and Poon W C K 2005 *Eur. Phys. J.* E **16** 77–80
[160] Babu S, Gimel J C and Nicolai T 2006 *J. Chem. Phys.* **125** 4512
[161] Witman J E and Wang Z G 2006 *J. Phys. Chem.* B **110** 6312
[162] Sastry S 2000 *Phys. Rev. Lett.* **85** 590–3
[163] Ashwin S S, Menon G I and Sastry S 2006 *Europhys. Lett.* **75** 922–8

[164] Bianchi E, Zaccarelli E, Sciortino F and Tartaglia P 2007 in preparation
[165] Ramakrishnan S, Fuchs M, Schweizer K S and Zukoski C F 2002 *J. Chem. Phys.* **116** 2201–12
[166] Shah S A, Chen Y L, Schweizer K S and Zukoski C F 2003 *J. Chem. Phys.* **118** 3350–60
[167] Segrè P N, Prasad V, Schofield A B and Weitz D A 2001 *Phys. Rev. Lett.* **86** 6042–5
[168] Jansen J W, De Kruif C G and Vrij A 1986 *J. Colloid Interface Sci.* **114** 481
[169] Lu P J, Conrad J C, Wyss H M, Schofield A B and Weitz D A 2006 *Phys. Rev. Lett.* **96** 028306
[170] Zaccarelli E, Löwen H, Wessels P P F, Sciortino F, Tartaglia P and Likos C N 2004 *Phys. Rev. Lett.* **92** 225703
[171] Vliegenthart G A and Van Der Schoot P 2003 *Europhys. Lett.* **62** 600–6
[172] Pierleoni C, Addison C, Hansen J P and Krakoviack V 2006 *Phys. Rev. Lett.* **96** 128302
[173] Lu P J, Ciulla F, Zaccarelli E, Trappe V, Schofield A B, Sciortino F and Weitz D A 2007 in preparation
[174] Cardinaux F, Stradner A, Schurtenberger P, Sciortino F and Zaccarelli E 2007 *Europhys. Lett.* **77** 48804
[175] Groenewold J and Kegel W K 2004 *J. Phys.: Condens. Matter* **16** 4877
[176] Sedgwick H, Egelhaaf S U and Poon W C K 2004 *J. Phys.: Condens. Matter* **16** 4913
[177] Sanchez R and Bartlett P 2005 *J. Phys.: Condens. Matter* **17** 3551
[178] Dibble C J, Kogan M and Solomon M J 2006 *Phys. Rev.* E **74** 041403
[179] Gao Y and Kilfoil M L 2007 *Phys. Rev. Lett.* at press
[180] Baglioni P, Fratini E, Lonetti B and Chen S H 2004 *J. Phys.: Condens. Matter* **16** S5003–22
[181] Stradner A, Cardinaux F and Schurtenberger P 2006 *J. Phys. Chem.* B **110** 21222
[182] Imperio A and Reatto L 2004 *J. Phys.: Condens. Matter* **16** 3769
[183] Coniglio A, De Arcangelis L, Del Gado E, Fierro A and Sator N 2004 *J. Phys.: Condens. Matter* **16** S4831–9
[184] Wu J, Liu Y, Chen W R, Cao J and Chen S 2004 *Phys. Rev.* E **70** 050401
[185] Tarzia M and Coniglio A 2006 *Phys. Rev. Lett.* **96** 075702
Tarzia M and Coniglio A 2007 *Phys. Rev.* E **75** 011410
[186] Liu Y, Chen W R and Chen S 2005 *J. Chem. Phys.* **122** 044507
[187] Wu J and Cao J 2006 *Physica* A **371** 249–55
[188] de Candia A, Del Gado E, Fierro A, Sator N, Tarzia M and Coniglio A 2006 *Phys. Rev.* E **74** 010403
[189] Pini D, Parola A and Reatto L 2006 *J. Phys.: Condens. Matter* **18** 2305
[190] Archer A, Pini D, Evans R L and Reatto L 2007 *J. Chem. Phys.* **126** 014104
[191] Allahyarov E, Zaccarelli E, Sciortino F, Tartaglia P and Loewen H 2007 *Europhys. Lett.* **78** 38002
[192] Vliegenthart G A, Lodge J and Lekkerkerker H N W 1999 *Physica* A **263** 378
[193] Renard D, Axelos M A V, Lefebvre J and Boue F 1995 *Biopolymers* **39** 149–59
[194] Le Bon C, Nicolai T and Durand D 1999 *Int. J. Food Sci. Technol.* **34** 451
[195] Pouzot M, Nicolai T, Durand D and Benyahia L 2004 *Macromolecules* **37** 614–20
[196] Grousson M, Tarjus G and Viot P 2000 *Phys. Rev.* E **62** 7781
[197] Löw U, Emery V J, Fabricius K and Kivelson S A 1994 *Phys. Rev. Lett.* **72** 1918
[198] Schmaliam J and Wolynes P 2000 *Phys. Rev. Lett.* **85** 836
[199] Wu D, Chandler D and Smit B 1992 *J. Phys. Chem.* **96** 4077–83
[200] Sear R P, Chung S, Markovich G, Gelbart W M and Heath J R 1999 *Phys. Rev.* E **59** 6255
[201] Lorenzana J, Castellani C and Castro C D 2001 *Phys. Rev.* B **64** 235127
[202] Likos C N, Mayer C, Stiakakis E and Petekidis G 2005 *J. Phys.: Condens. Matter* **17** 3363
[203] Bernal J D 1964 *Proc. R. Soc.* A **299** 280
[204] Deem M W and Chandler D 1994 *Phys. Rev.* E **49** 4276–85
[205] Sear R P and Gelbart W M 1999 *J. Chem. Phys.* **110** 4582–8
[206] Tanaka H, Meunier J and Bonn D 2004 *Phys. Rev.* E **69** 031404
[207] Mongondry P, Tassin J and Nicolai T 2005 *J. Colloid Interface Sci.* **283** 397–405
[208] Ruzicka B, Zulian L and Ruocco G 2006 *Langmuir* **22** 1106
[209] Ruzicka B, Zulian L and Ruocco G 2004 *J. Phys.: Condens. Matter* **16** 4993
[210] Shalkevich A, Stradner A, Bhat S K, Muller F and Schurtenberger P 2007 *Langmuir* **23** 3570
[211] Bordi F, Cametti C, Gili T, Gaudino D and Sennato S 2003 *Bioelectrochemistry* **59** 99–106
[212] Bordi F, Cametti C, Diociaiuti M, Gaudino D, Gili T and Sennato S 2004 *Langmuir* **20** 5214–22
[213] Bordi F, Cametti C, Diociaiuti M and Sennato S 2005 *Phys. Rev.* E **71** 050401
[214] Bordi F, Cametti C and Sennato S 2005 *Chem. Phys. Lett.* **409** 134
[215] Stiakakis E, Petekidis G, Vlassopoulos D, Likos C N, Iatrou H, Hadjichristidis N and Roovers J 2005 *Europhys. Lett.* **72** 664–70
[216] Mladenovic I, Kegel W, Bomans P and Frederik P 2003 *J. Phys. Chem.* B **107** 5717
[217] Validzic I L, van Hooijdonk G, Oosterhout S and Kegel W 2004 *Langmuir* **20** 3435
[218] Hoffmann N, Ebert F, Likos C N, Löwen H and Maret G 2006 *Phys. Rev. Lett.* **97** 078301
[219] Pan W C, Galkin O, Filobelo L, Nagel R L and Vekilov P G 2006 *Biophys. J.* **92** 267

[220] Boutet S and Robinson I K 2007 *Phys. Rev.* E **75** 021913
[221] Mladek B M, Gottwald D, Kahl G, Neumann M and Likos C N 2006 *Phys. Rev. Lett.* **96** 045701
[222] Yi G R, Manoharan V N, Michel E, Elsesser M T, Yang S and Pine D J 2004 *Adv. Mater.* **16** 1204–7
[223] Klein S M, Manoharan V N, Pine D J and Lange F F 2005 *Langmuir* **21** 6669–74
[224] Cho Y S, Yi G R, Lim J M, Kim S H, Manoharan V N, Pine D J and Yang S M 2005 *J. Am. Chem. Soc.* **127** 15968–75
[225] Liddell C M and Summers C J 2003 *Adv. Mater.* **15** 1715–9
[226] Zerrouki D, Rotenberg B, Abramson S, Baudry J, Goubault C, Leal-Calderon F, Pine D J and Bibette J 2006 *Langmuir* **22** 57–62
[227] Zhang G, Wang D and Möhwald H 2005 *Angew. Chem. Int. Edn* **44** 1–5
[228] Whitesides G M and Boncheva M 2002 *Proc. Natl Acad. Sci.* **99** 4769–74
[229] Glotzer S C 2004 *Science* **306** 419–20
[230] Zhang Z, Horsch M A, Lamm M H and Glotzer S C 2003 *Nano Lett.* **3** 1341–6
[231] Zhang Z and Glotzer S C 2004 *Nano Lett.* **4** 1407–13
[232] Glotzer S C, Solomon M J and Kotov N A 2004 *AIChE J.* **50** 2978
[233] Zhang Z, Keys A S, Chen T and Glotzer S C 2005 *Langmuir* **21** 11547
[234] Wilber A W, Doye J P K, Louis A A, Noya E G, Miller M A and Wong P 2006 *Preprint* cond-mat/0606634
[235] Kalsin A M, Fialkowski M, Paszewski M, Smoukov S K, Bishop K J M and Grzybowski B A 2006 *Science* **312** 420–4
[236] Maldovan M and Thomas E 2004 *Nat. Mater.* **3** 593–600
[237] Lu Y, Yin Y and Xia Y 2001 *Adv. Mater.* **13** 415
[238] Doye J P K, Louis A A, Lin I, Allen L R, Noya E G, Wilber A W, Chwan Kok H and Lyus R 2007 *Phys. Chem. Chem. Phys.* **9** 2197
[239] Rechtsman M C, Stillinger F H and Torquato S 2005 *Phys. Rev. Lett.* **95** 228301
[240] Rechtsman M, Stillinger F and Torquato S 2006 *Phys. Rev.* E **73** 011406
[241] Rechtsman M C, Stillinger F H and Torquato S 2006 *Phys. Rev.* E **74** 021404
[242] Kern N and Frenkel D 2003 *J. Chem. Phys.* **118** 9882–9
[243] Lomakin A, Asherie N and Benedek G B 1999 *Proc. Natl Acad. Sci.* **96** 9465–8
[244] Sear R P 1999 *J. Chem. Phys.* **111** 4800–6
[245] Zaccarelli E, Saika-Voivod I, Moreno A J, Buldyrev S V, Tartaglia P and Sciortino F 2006 *J. Chem. Phys.* **124** 124908
[246] Speedy R J and Debenedetti P G 1994 *Mol. Phys.* **81** 237
[247] Speedy R J and Debenedetti P G 1996 *Mol. Phys.* **88** 1293
[248] Moreno A J, Buldyrev S V, La Nave E, Saika-Voivod I, Sciortino F, Tartaglia P and Zaccarelli E 2005 *Phys. Rev. Lett.* **95** 157802
[249] Moreno A J, Saika-Voivod I, Zaccarelli E, Nave E L, Buldyrev S V, Tartaglia P and Sciortino F 2006 *J. Chem. Phys.* **124** 204509
[250] Zaccarelli E, Saika-Voivod I, Moreno A J, Nave E L, Buldyrev S V, Tartaglia P and Sciortino F 2006 *J. Phys.: Condens. Matter* **18** S2373
[251] Corezzi S *et al* 2007 in preparation
[252] Kolafa J and Nezbeda I 1987 *Mol. Phys.* **61** 161–75
[253] Nezbeda I, Kolafa J and Kalyuzhnyi Y V 1989 *Mol. Phys.* **68** 143–60
[254] Nezbeda I and Iglesia-Silva G 1990 *Mol. Phys.* **69** 767–74
[255] Sear R P and Jackson J G 1996 *J. Chem. Phys.* **105** 1113–20
[256] Vega C and Monson P A 1998 *J. Chem. Phys.* **109** 9938–49
[257] Ford M H, Auerbach S M and Monson P A 2004 *J. Chem. Phys.* **121** 8415–22
[258] Wertheim M 1984 *J. Stat. Phys.* **35** 19
Wertheim M 1984 *J. Stat. Phys.* **35** 35
Wertheim M 1986 *J. Chem. Phys.* **85** 2929
[259] De Michele C, Gabrielli S, Tartaglia P and Sciortino F 2006 *J. Phys. Chem.* B **110** 8064
[260] de Michele C, Tartaglia P and Sciortino F 2006 *J. Chem. Phys.* **125** 4710
[261] Del Gado E and Kob W 2005 *Europhys. Lett.* **72** 1032–8
[262] Del Gado E and Kob W 2007 *Phys. Rev. Lett.* **98** 028303
[263] Sciortino F, Bianchi E, Douglas J and Tartaglia P 2007 *J. Chem. Phys.* **126** 194903
[264] Blaak R, Miller M and Hansen J 2007 *Europhys. Lett.* **78** 26002
[265] Hiddessen A L, Rotgers S D, Weitz D A and Hammer D A 2000 *Langmuir* **16** 9744–53
[266] Hiddessen A L, Weitz D A and Hammer D A 2004 *Langmuir* **20** 71–104
[267] Mirkin C A, Letsinger R L, Mucic R C and Storhoff J J 1996 *Nature* **382** 607–9

[268] Valignat M P, Theodoly O, Crocker J C, Russel W B and Chaikin P M 2005 *Proc. Natl Acad. Sci.* **102** 4225
[269] Lukatsky D B and Frenkel D 2004 *Phys. Rev. Lett.* **92** 068302
[270] Lukatsky D B, Mulder B M and Frenkel D 2006 *J. Phys.: Condens. Matter* **18** 567
[271] Starr F W and Sciortino F 2006 *J. Phys.: Condens. Matter* **18** L347–53
[272] Largo J, Starr F W and Sciortino F 2007 *Langmuir* **23** 5896
[273] Largo J, Tartaglia P and Sciortino F 2007 *Preprint* cond-mat/0703383
[274] Adam M and Lairez D 1996 *The Physical Properties of Polymeric Gels* (New York: Wiley) p 87
[275] Sciortino F and Tartaglia P 1995 *Phys. Rev. Lett.* **74** 282–5
[276] Cipelletti L, Manley S, Ball R C and Weitz D A 2000 *Phys. Rev. Lett.* **84** 2275–8
[277] Pini D, Ge J L, Parola A and Reatto L 2000 *Chem. Phys. Lett.* **327** 209
[278] Ren S Z and Sorensen C M 1993 *Phys. Rev. Lett.* **70** 1727–30
[279] Broderix K, Goldbart P M and Zippelius A 1997 *Phys. Rev. Lett.* **79** 3688–91
[280] Elliott S L, Butera R J, Hanus L H and Wagner N J 2003 *Faraday Discuss.* **123** 369–83
[281] Krall A H and Weitz D A 1998 *Phys. Rev. Lett.* **80** 778–81
[282] Rueb C J and Zukoski C F 1998 *J. Rheol.* **42** 1451
[283] Prasad V, Trappe V, Dinsmore A D, Segre P N, Cipelletti L and Weitz D A 2003 *Faraday Discuss.* **123** 1–12
[284] Trappe V, Prasad V, Cipelletti L, Segre P N and Weitz D A 2001 *Nature* **411** 772–5
[285] Mattson J *et al* 2007 in preparation
[286] Weeks E R, Crocker J C, Levitt A C, Schofield A and Weitz D A 2000 *Science* **287** 627–31
[287] Bissig H, Romer S, Cipelletti L, Trappe V and Schurtenberger P 2003 *Phys. Chem. Commun.* **6** 21
[288] Puertas A, Fuchs M and Cates M E 2004 *J. Chem. Phys.* **121** 2813–22
[289] Coniglio A, Abete T, de Candia A, Del Gado E and Fierro A 2007 *J. Phys.: Condens. Matter* **19** 205103
[290] Doye J P K and Poon W C K 2006 *Curr. Opin. Colloid Interface Sci.* **11** 40